**The Thesis Committee for Paul Joseph Ruess**
**Certifies that this is the approved version of the following thesis:**

# Height Above Nearest Drainage: Assessment and Recommendations for Improved Rating Curve Generation

**APPROVED BY**
**SUPERVISING COMMITTEE:**

**Supervisor:**

David R. Maidment

Paola Passalacqua

# Height Above Nearest Drainage: Assessment and Recommendations for Improved Rating Curve Generation

**by**

**Paul Joseph Ruess, B.S.**

**Thesis**

Presented to the Faculty of the Graduate School of

The University of Texas at Austin

in Partial Fulfillment

of the Requirements

for the Degree of

**Master of Science in Engineering**

**The University of Texas at Austin**

**May 2017**

# Acknowledgements

Thank you first and foremost to Dr. David R. Maidment, whose unwavering compassion and persistent pursuit of knowledge has finally culminated in the conception of a feasible methodology for widespread flood prediction. Without the extensive research progress made by Dr. Maidment and his contemporaries over the past decades, this research and its potential implications would never have been possible. I truly am walking alongside a giant, and for this experience I am eternally grateful.

Secondly, and certainly not least, I would like to extend my thanks to Xing Zheng for his selfless dedication to this research. This work was largely made possible due to Xing's previous research and many methodologies which he developed along the way. Thank you for struggling through some of my most difficult problems with me, and for helping guide the direction of this work.

I would also like to thank our entire research team at the Center for Research in Water Resources. In particular, thank you to Dr. Paola Passalacqua and Dr. Tim Whiteaker for your recommendations throughout the progression of this research.

Finally, I would like to thank the Consortium of Universities for the Advancement of Hydrologic Science, Inc. for sponsoring me as a Graduate Research Fellow at the National Water Center Summer Institute of 2016.

# Abstract

## Height Above Nearest Drainage: Assessment and Recommendations for Improved Rating Curve Generation

Paul Joseph Ruess, M.S.E.

The University of Texas at Austin, 2017

Supervisor: David R. Maidment

Real-time flood forecasting for the Conterminous United States is currently underway. Powered by improvements to the Height Above Nearest Drainage methodology, coupled with the recent publication of streamflow predictions through the National Water Model, few uncertainties remain before implementation can be realized. Of these uncertainties, rating curve generalizations for all NHDPlusV2 stream reaches in the nation has persistently proven problematic, particularly regarding approximations of Manning's roughness and stream reach slope values. This research attempts to address these concerns through detailed analyses of various rating curves along Onion Creek in Austin, Texas. From this research, alternatives are proposed to the currently used roughness and slope values, and the overall performance of these alternatives is assessed to provide recommendations for future rating curve approximations.

# Table of Contents

# List of Tables

# List of Figures

# Chapter 1: Introduction

## 1.1 Motivation

Flooding is the most impactful natural disaster worldwide: "since 1995, floods have accounted for 47% of all weatherrelated disasters, affecting 2.3 billion people" (Wahlstrom & Guha-Sapir, 2015). Specifically in the United States (U.S.), flooding accounts for 44% of the country's deaths caused by natural disasters, and the frequency of these deaths has persisted over the last decades with an average of 102 annual deaths (Figure 1) (NWS, 2016). More work is necessary to effectively address this need.

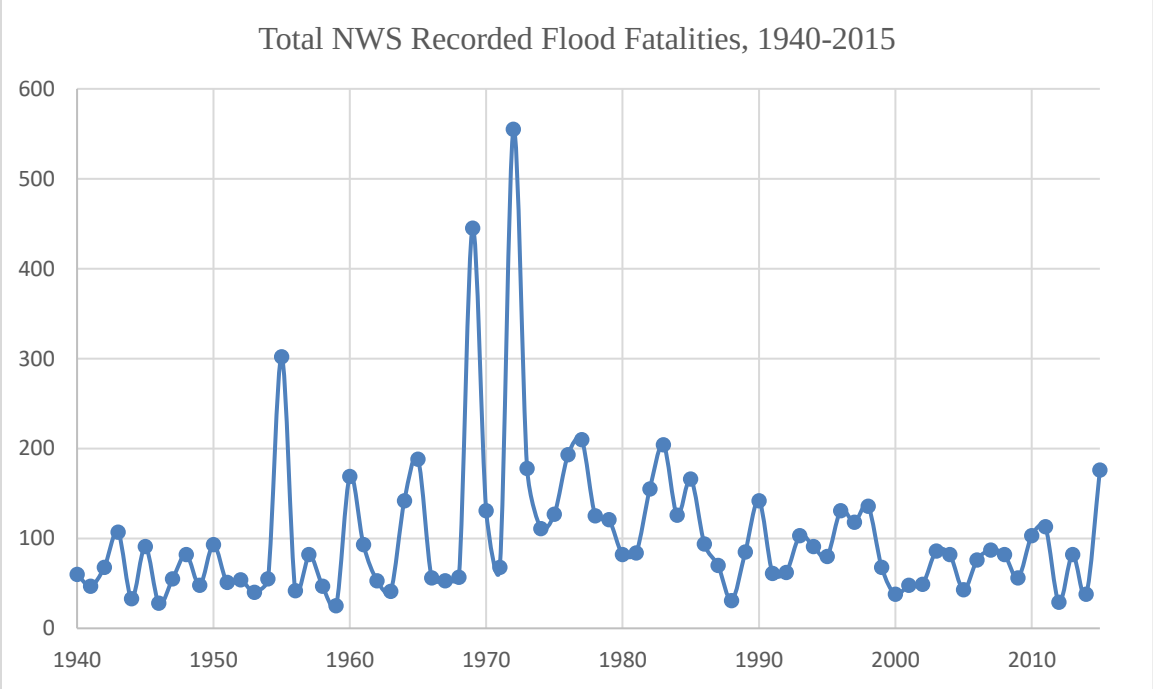


Figure 1: Annual flood fatalities as reported by the National Weather Service's National Hazard Statistics dataset (NWS, 2016).

## 1.2 Background

In response to the large number of annual flood deaths, the National Weather Service (NWS) River Forecast System (RFS) was created. The RFS produces flood

forecasts at approximately 3,600 larger streams and rivers throughout the United States, including Alaska and Hawaii (NWS, n.d.). Additional work by the Federal Emergency Management Agency (FEMA) has systematically compiled FEMA National Flood Insurance Program flood hazard maps into a digital database, the National Flood Hazard Layer (NFHL) (FEMA, n.d.). The NFHL enables access to flood risks maps for approximately 60% of the land area and 88% of the area in the United States (Maidment, 2016). However, despite these efforts, flood deaths continue to occur throughout the U.S., with 176 reported flash flood and/or river flood fatalities in 2015 (NWS, n.d.).

Recent efforts at improving upon the RFS and NFHL have led to the development of the National Water Model (NWM). The NWM was released on August 16, 2016 through a National Oceanic and Atmospheric Administration (NOAA) collaboration with the National Center for Atmospheric Research (NCAR), the Consortium of Universities for the Advancement of Hydrologic Sciences (CUAHSI), the National Science Foundation (NSF), and federal Integrated Water Resources Science and Services Consortium partners (NOAA, 2016). Through this collaboration, the NWM has become a very complete predictive force, significantly improving detailed understandings of America's waters. The NWM in particular tremendously enables future efforts for flood forecasting through the production of streamflow predictions.

Using NWM streamflow predictions, two final conversions must be realized for generating flood forecasts. First, these forecast discharges must be converted to stage heights. Once stage heights are calculated, a second conversion is needed to translate from a stage height to a flood extent.

The streamflow to stage height conversion is traditionally accomplished through the use of rating curves, specifically a stage-discharge rating curve (Sauer, 2002). According to the Office of Water Prediction, "all [NWM] configurations provide

streamflow for 2.7 million river reaches and other hydrologic information on 1km and 250m grids" (Cosgrove & Klymmer, 2016). As such, once a rating curve is known for each stream reach, discharged provided by the NWM can be used to programmatically predict flood extents for the entire nation. This is the true objective, and justification for, this particular research.

These stage-discharge rating curves are usually generalized through frequent and highly-detailed field measurements. A leader in U.S. field measurement collection and subsequent rating curve creation is the United States Geological Survey (USGS), providing rating curves for many thousands of stream reaches in the Conterminous United States (CONUS) (USGS, n.d.). Additional rating curve data can be generated through the use of local Hydrologic Engineering Center River Analysis System (HEC-RAS) models (Brunner, 2016); this methodology will later be explored in detail.

Stage height to flood extent conversions are outside the scope of this work, but it is still valuable to briefly mention them. While various options exist for mapping flood extents, the shortage here is in generalized methodologies that enable instantaneous predictive flood mapping strictly from stage-height and terrain data. In response to this need, ongoing research applying the Height Above the Nearest Drainage (HAND) methodology to flood mapping is underway (Liu et al., 2016; Liu, Maidment, Tarboton, Zheng, & Wang, 2017).

Notably, the HAND methodology has additional applications in rating curve generation at large scales (Zheng, Tarboton, Maidment, Liu, & Passalacqua, 2017), potentially enabling accurate rating curve approximations to be constructed for all 2.67 million National Hydrography Dataset Plus Version 2 (NHDPlusV2) stream reaches in the nation (Mckay et al., 2012). This work has already been accomplished, however it relies on the tremendous assumption that Manning's roughness coefficient is 0.05 for all stream

reaches in the nation, effectively ignoring the physical characteristics of the stream reach (Zheng et al., 2017). As will be further observed, NHDPlusV2 slope values for Onion Creek are also highly variable, presenting additional room for improvement.

Owing to the existence of current pitfalls to the HAND method, this work focuses on introducing potential improvements to these faults. More specifically, this work serves as a study of HAND, USGS, and HEC-RAS rating curves and cross-sections, focused on understanding how the HAND methodology can be improved to more closely align with generally accepted USGS and HEC-RAS hydraulics. Ideally these improvements will inform future HAND development to better approximate reality, in turn enhancing the accuracy of HAND-based flood extent forecasts.

Once these corrections are resolved, HAND flood extents will hopefully be published by the NWS as authoritative flood extent predictions. Using these authoritative, publicly-available predictions, forecast dissemination tools will be used to communicate forecast flood extents to first responders and citizens. Preliminary work in this area has been investigated, creating highly-detailed engineering-grade flood forecasts and communicating these results to the local first response communities around Austin, Texas (Fagan, 2016). Further work along this vein proposed the OPERA prototype, extending the responsibilities of first responders to the public and enabling individuals to inform themselves through social media flood alert integration (Johnson, Ruess, & Coll, 2016).

### 1.3 Overview

Ultimately, the goal of this research is to improve the accuracy of HAND forecast flood extents as much as possible before passing them off to the NWS for widespread, real-time, dynamic flood-mapping services intended to decrease flood deaths nation-wide. HAND improvements are particularly sought in the form of improved rating curves,

specifically through the replacement of the existing Manning's roughness coefficient assumption (n = 0.05) with more informed Manning's roughness values. An additional area requiring further improvement is in the derivation of improved slopes as compared to NHDPlusV2 stream reach slopes; this is explored in this work, yet further work is required before conclusive results can be arrived at. Overall, the contributions realized by this work are presented as potentially generalizable corrections to the Manning's roughness and slope used in computing HAND rating curves. Through these corrections, HAND rating curves are intended to more accurately represent the channels which they describe, significantly improving the conversion from NWM discharges to stage heights. Improvements to this conversion consequently better flood extent prediction accuracy overall, potentially decreasing loss of life.

# Chapter 2: Literature Review

## 2.1 Hydraulic Geometry

First introduced in 1953, Hydraulic Geometry (HG) has been an on-going area of research to understand seemingly consistent mathematical relationships relating river geometries to mean annual discharge (Leopold & Maddock, 1953). Two different forms of HG were introduced, namely at-a-station hydraulic geometries (AHG) and downstream hydraulic geometries (DHG). AHG speaks to relationships between instantaneously-measured channel geometries (namely width, depth, and velocity) and discharge. Similarly, DHG relates measured cross-sectional geometries downstream of a station to the mean annual discharge for that cross section. These initial investigations showed that power law trends relating mean annual discharge to width, to depth, and to velocity were independently existent for various rivers in the western U.S, and these relationships were respectfully described by the following equations:

$$w = aQ^b$$

$$d = cQ^f$$

$$v = kQ^m$$

Interestingly, as was observed by Leopold and Maddock, Q = wdv results in these equations all being constrained by their units: $a$ x $c$ $x$ k must equal 1, and $b + f + m$ must also equal 1. Additional research by both Parker (1977) and Rhodes (1977) independently concluded that AHG exponents experience spatial variation. Both Parker (1977) and Rhodes (1977) used a ternary diagram to assess these similarities, an example of which is shown in Figure 2.

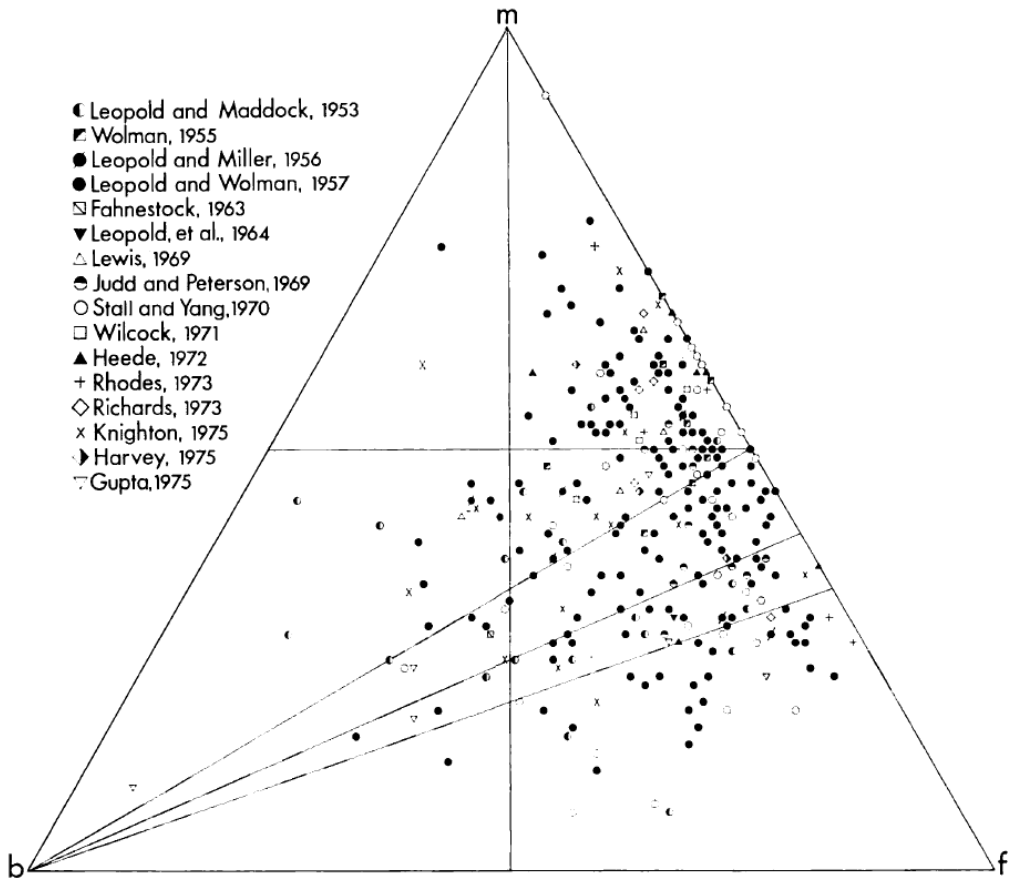


Figure 2: Ternary diagram displaying *b*, *f*, and *m* exponents for 315 AHG data points (some points overlap with others) (Rhodes, 1977).

Further investigations by Knighton (1974, 1975) extended this line of thought, successfully identifying that similar power law relationships exist, relating discharge to suspended sediment, flow resistance, bed slope, Manning's *n*, and the Darcy-Weisbach *f*. Knighton (1975) further showed that, while AHG varies spatially, temporal variations exist as well; this conclusion was arrived at through a study of changes in AHG-derived slopes over time.

One of the most impactful studies of this ongoing AHG research is an article published by Ferguson (1986). Using widely accepted flow resistance equations, Ferguson

(1986) successfully derived AHG values for different channel geometries, essentially by-passing the need to use width, depth, velocity, and discharge data typically collected in the field. Ferguson (1986) also claimed that the power law form so often identified as authoritative was in fact strictly coincidental.

The former of these two findings is arguably the more important, particularly as it applies to the work here presented. According to Ferguson (1986), Manning's equation (described in the "Rating Curve" section) can be used to determine velocity as a function of a cross section's depth. This derived velocity can then be combined with the Keulegan flow law to arrive at a width-to-depth relationship (Gleason, 2015; Hijar, 2015).

### 2.2 Height Above the Nearest Drainage

Continuing along the same stream of thought, the Height Above the Nearest Drainage (HAND) model was initially constructed as a Digital Elevation Model (DEM)-based terrain model intended for terrain classification between soil water conditions and topography based on soil drainage potential (Rennó et al., 2008). Further research has expanded upon (Nobre et al., 2011) and implemented the HAND model for various purposes, such as landscape classification (Gharari, 2011) and flood extent modeling (Liu et al., 2016; Liu et al., 2017). Similar conceptually to the HG methodologies – particularly as developed and described by Ferguson (1986) – HAND is now being used to develop river channel properties (ie. hydraulic geometries), enabling a detailed understanding of all river reaches in the CONUS.

In more detail, the HAND methodology determines the height value for each 10m x 10m raster grid-cell based on that cell's nearest stream reach, determined by following the path of steepest descent using a 10m x 10m DEM (the 10m x 10m size selection was a result of the National Elevation Dataset (NED) which is being used in this analysis). As a

result, a HAND raster represents the stage height requirement for each grid-cell in a catchment to become inundated. For example, a HAND value of 20 feet means that the grid-cell in question is 20 feet above its nearest stream reach. This means that once the stream reaches a stage height of 20 feet, that particular grid-cell will become inundated.

Specifically pertaining to flood forecasting, HAND presents a new approach for flood inundation mapping in a computationally efficient way, relying effectively on a NED DEM that has been normalized to its respective watershed (Liu et al., 2016; Liu et al., 2017). This enables HAND data to be collected and organized in a raster format (a matrix where each cell contains associated values) collected from DEMs. These HAND rasters can then be stored for quick access, bypassing any hydraulic calculations that would otherwise be necessary for generating an inundation map (assuming stage height is provided). Consequently, the HAND methodology is intended primarily for flood inundation mapping (ie. given a stage-height, a flood extent map can be produced by showing which grid-cells are inundated). However, by using an assumed maximum depth, the HAND method can also be used to approximate various hydraulic properties for each depth interval therein (Zheng et al., 2017).

The data needed to construct a HAND rating curve is the following: the wetted area, hydraulic radius, channel bed-slope, and Manning's roughness. Using an assumed stage height, the approximate channel width can be derived from a HAND flood extent and the wetted area can then be computed. While this is not the same as the approach proposed by Ferguson (1986) to compute channel geometries, the end result is identical: using a HAND raster, various channel geometries can be back-calculated from the terrain data.

Using the wetted area previously computed and assuming a trapezoidal geometry, the hydraulic radius can further be computed using this same channel width in addition to the channel length, which is retrievable from the NHDPlusV2 dataset. Slope is also

contained in the NHDPlusV2 dataset, leaving the Manning's roughness coefficient as the only unknown parameter for converting between stage and discharge. While hydraulic geometries computed through typical AHG methodologies may have enabled the computation of these slopes, the lack of a solid theoretical understanding of the underlying mechanisms driving HGs to work was seen as good reason not to rely on their application. Additionally, seeing as there was no existing method available for generalizing Manning's roughness on a national scale for all NHDPlusV2 stream reaches (in a proven and reliable way, excluding HG approaches), this Manning's roughness coefficient was assumed to be 0.05 everywhere. This assumption, along with the derived channel geometries, made the computation of HAND-derived rating curves for all 2.67 million stream reaches possible.

While this methodology is relatively sound, the accuracy of HAND-derived rating curves is questionable due to DEM imperfections. DEMs are generally constructed with the use of remote sensing technologies which often fail to penetrate through water surfaces; this technology is currently advancing, but the construction of accurate bathymetric data from DEMs is still in progress (Hernandez & Armstrong, 2016). This discrepancy introduces potentially faulty errors to the HAND-based rating curves created in this way. Further complications arise due to the Manning's roughness assumption of 0.05 for all streams, which clearly ignores the physical characteristics of the stream, decreasing the completeness and accuracy of this approach.

### 2.3 National Water Model

The release of the NWM now provides a myriad of hydrological and atmospheric water-related forecasts for the 2.67 million stream reaches in the NHDPlusV2 dataset (Mckay et al., 2012), which approximately represents all stream reaches throughout the CONUS (Cosgrove & Klymmer, 2016). These forecasts exist in various scenarios,

collectively accounting for up to thirty-day forecasts and refresh frequencies as small as every hour (Cosgrove & Klymmer, 2016). In addition to the release of this incredible dataset, relatively simple methods exist for accessing this data through the National Water Model Forecast Viewer and its associated Application Program Interface (published through a HydroShare (Tarboton et al., 2014) web application, which requires a free account to access) (NWM Forecast Viewer, 2016). A python wrapper for easily retrieving large series of these forecasts also exists (Whiteaker, 2016).

In terms of providing flood forecasts, the most practical outputs from the NWM are the various channel streamflow forecasts available. With these streamflow forecasts and their associated forecast timestamps, a predictive hydrograph can be generated for any of the ~2.67 million stream reaches in the CONUS, up to thirty days into the future. Figure 3 shows an example of a five-day forecast retrieved on March 17, 2017 at 3:00 pm using the National Water Model Forecast Viewer HydroShare application (NWM Forecast Viewer, 2016).

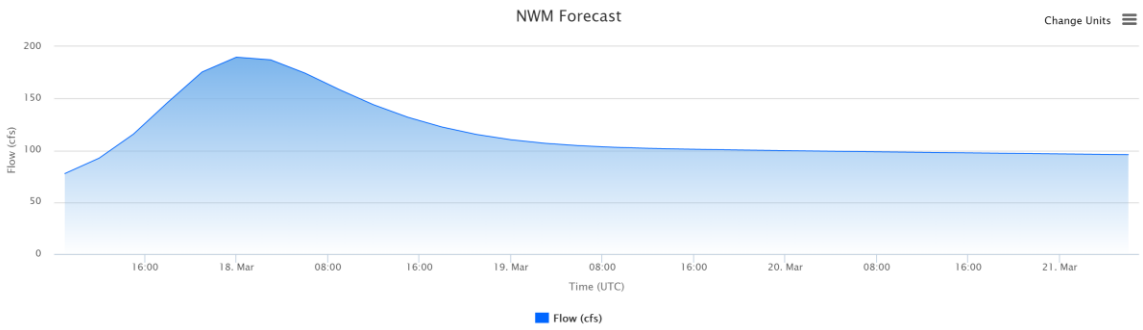


Figure 3: Hydrograph forecast for Onion Creek at Highway 183 in Austin, Texas.

## 2.4 Rating Curves

Before exploring available HAND, USGS, and HEC-RAS data, an introduction to the rating curve methodologies here used is necessary. A rating curve can describe many

different surface water relationships (Sauer, 2002). In this work, the most common rating curve will be used: the relationship between volumetric discharge (ie. streamflow) and river stage height (ie. height of a river measured above the lowest point in a cross-section) for any given stream reach.

Rating curves have been studied for many years and are consequently accepted as the standard streamflow-to-flood-depth conversion. Historically, Manning's equation has been used to generate rating curves, relying on empirically-derived relationships between physical channel properties and the Manning's roughness coefficient (Manning, 1895). The weakness to this approach is the dependency on a prescribed channel description, such as a stream being natural, clean, and straight resulting in a Manning's roughness of n = 0.03 (Chow, Maidment, & Mays, 1988). This dependency leads to different rating curves based on different observers' assessments of a channel's roughness. An additional weakness is that this prescriptive approach leads to rating curves going unchecked and subsequently having consistent roughness values over long periods of time (despite the fact that, particularly after large flooding events, terrain can shift and often cause a rating curve to change).

While rating curves accomplish their task well, it is important to note two major dependencies that impact their applicability. First-off, a constant stage-discharge relationship must exist at a cross section for a rating curve to be valid. Due to scour and deposition, seasonal variation of aquatic vegetation, variable backwater effects, and ice, streams may change significantly, requiring changes to the existent rating curve (Braca & Futura, 2008). In some special cases rating curves may even need to be divided into two pieces, with a low and a high flow component, in order to actually be valid (Braca & Futura, 2008). While this last point is important, it cannot be realized by the current HAND rating curves, and therefore will not be considered in this analysis.

A second dependency of rating curves is the requirement for steady flow, meaning that depth, water area, velocity, and discharge remain constant along the stream reach in question (Chow, 1953). While this can be a tremendous problem for USGS rating curves, which are available only at select river cross sections, HAND nullifies this concern by treating each stream reach as one entity. This means that HAND always assumes steady flow for all HAND rating curves, consequently avoiding any complications presented to rating curves by non-steady flow, such as hysteresis (Braca & Futura, 2008).

Though various open channel flow equations may be applicable (Chow, Maidment, & Mays, 1988), this project has elected to utilize the Manning's equation for simplicity and conformity reasons. The HAND approach currently in use relies on the Manning's approach for rating curve generation, and thus this approach will be used to explore these improvements. Notably, this research is not intended to investigate the correctness of the Manning's approach, it is simply intended to improve the accuracy of the HAND methodology for deriving rating curves. In order to explore potential improvements, HAND rating curves must be normalized against USGS and HEC-RAS rating curves, which also use the Manning's equation methodology (Brunner, 2016; USGS, n.d.). This consistent application of Manning's equation to all authoritative rating curve datasets mandates that this particular investigation use the same approach. Manning's equation is described as follows:

$$Q = \frac{k}{n} A_w H_R^{2/3} S_0^{1/2}$$

Where Q is the discharge [$L^3/T$]; $A_w$ is the cross-sectional wetted area [L2]; $H_R$ is the hydraulic radius [L]; $S_0$ is the channel bed slope at constant water depth [L/L]; n is the

so-called Manning's roughness coefficient [$T/L^{1/3}$]; and k is a conversion factor, 1.0 for SI units and 1.49 for English units (Manning, 1891). Consequently, using Manning's equation, a rating curve can only be created if the discharge and height (included in the area term) are related, requiring $A_w$, $H_R$, $S_0$, and n to be known.

# Chapter 3: Methodology

## 3.1 Preliminary Study Area

Initial studies were conducted in the Onion Creek watershed just South-west of Austin, Texas. This area is of particular interest due to the frequency of severe flooding in the area (Austin American-Statesman, n.d.). As seen in Figure 4, there are quite a few USGS gages and HEC-RAS cross sections within the Onion Creek watershed: local USGS gages are represented by the red "StreamGage" circles, HEC-RAS cross sections are represented by purple "XSLine_OnionCreek" lines, and blue lines represent the NHDPlusV2 stream reaches sized according to their mean annual flowrate ("Q0001C"). Importantly, this preliminary study area uses HEC-RAS cross sections from multiple Austin FloodPro HEC-RAS models which had been combined in a previous study (Zheng, 2015).

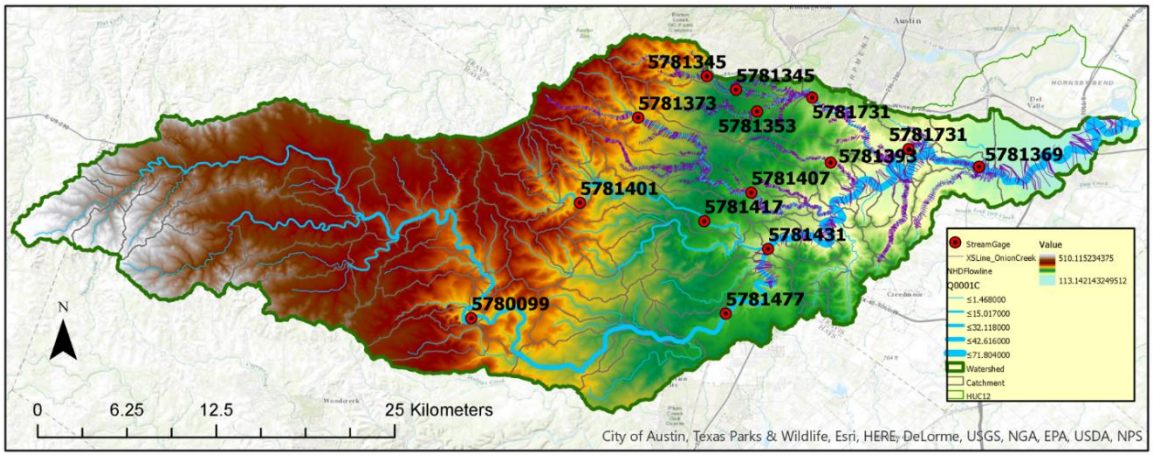


Figure 4: Preliminary study area representing the Onion Creek watershed.

In the preliminary analyses, three particular stream reaches were selected as a representative sample of the Onion Creek watershed; these three reaches are summarized in Table 1. One critical decision in the selection of these reaches was their large HEC-RAS

cross section density, enabling a more thorough analysis of HAND rating curves as compared to HEC-RAS data. These stream reaches also needed to approximately represent the range of variations present in the dataset, resulting in the selection of reaches of varying lengths, USGS stream gage locations, and topographical ranges.

| COMID | Stream Reach Length (ft) | USGS Stream Gage Location | # HEC-RAS Cross-sections | Topography Range (ft) |
|---|---|---|---|---|
| 5781369 | 15,521 | Downstream end | 63 | 62.538 |
| 5781373 | 25,803 | Upstream end | 102 | 127.212 |
| 5781407 | 32,175 | Middle | 105 | 100.718 |

Table 1: Summary of three selected stream reaches for preliminary analysis.

As an aid to generally understand these reaches prior to analyzing them, cartographic details for all of these reaches were generated in the form of 2-dimensional and 3-dimensional maps (see Figures 5, 6, and 7). These maps helped inform where the USGS gages were located along each stream reach as well as what the topography ranges were for each stream reach.

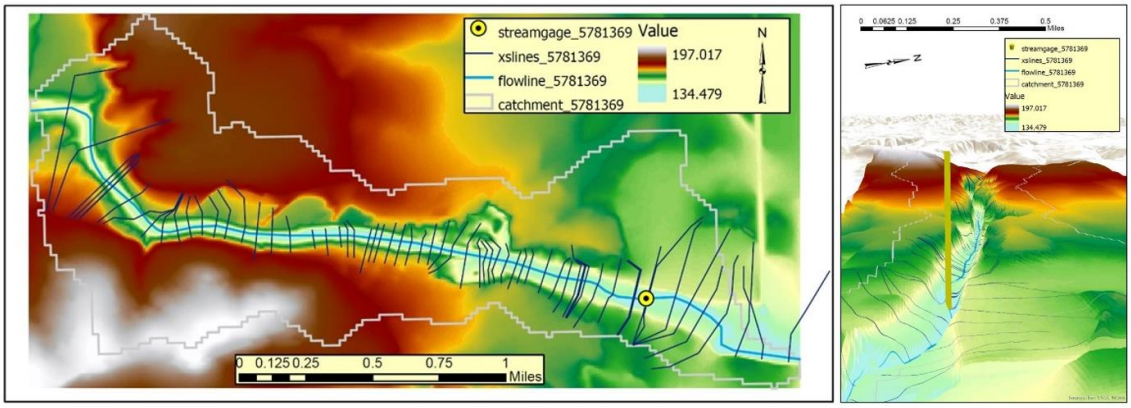


Figure 5: 2-Dimensional (left) and 3-Dimensional (right) maps of NHDPlusV2 COMID 5781369.

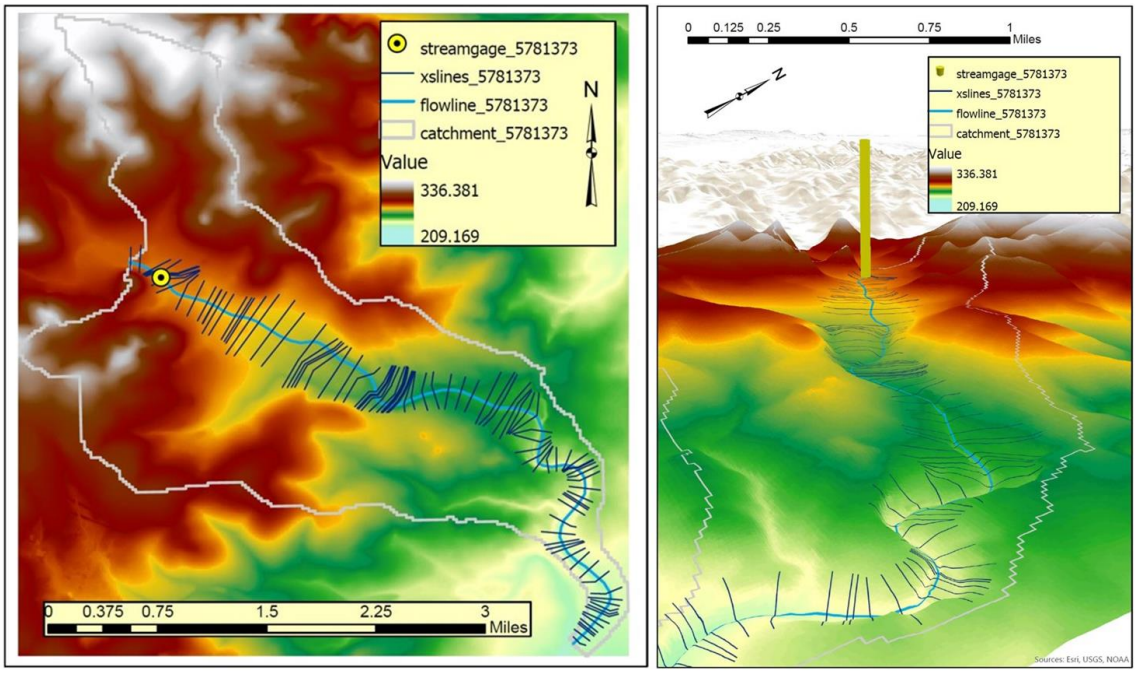


Figure 6: 2-Dimensional (left) and 3-Dimensional (right) maps of NHDPlusV2 COMID 5781373.

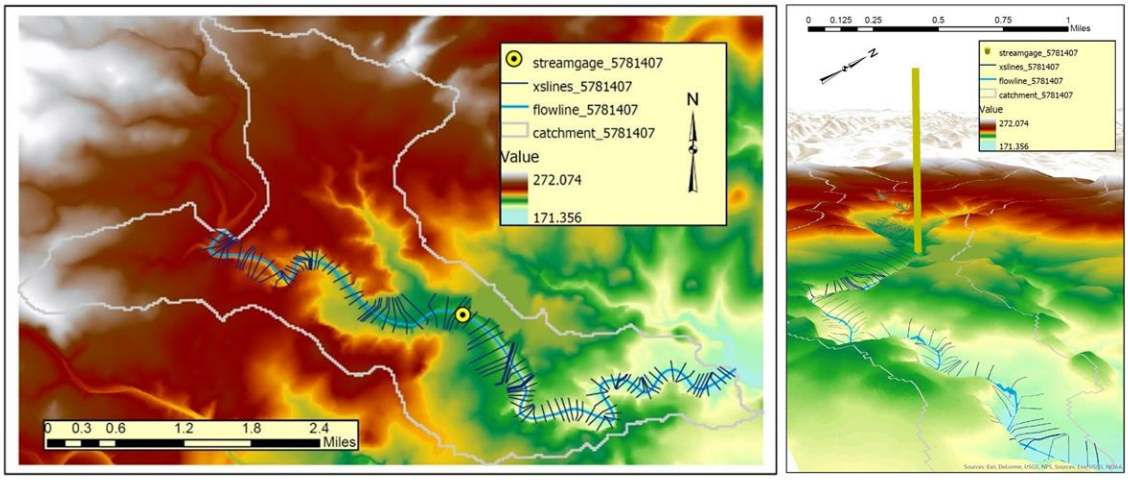


Figure 7: 2-Dimensional (left) and 3-Dimensional (right) maps of NHDPlusV2 COMID 5781407.

## 3.2 AVAILABLE DATA

This research relies primarily on two types of data along stream reaches: rating curves and transverse cross sections. Transverse cross sections were collected for HAND and USGS stream reaches primarily for preliminary analysis, after which the focus of this research turned strictly to rating curves. HEC-RAS cross-sections were also collected strictly with the purpose of converting them into HEC-RAS rating curves. Rating curve data was also gathered for HAND and USGS stream reaches.

### 3.2.1 National Hydrography Dataset Plus Version 2

The National Hydrography Dataset Plus Version 2 (NHDPlusV2) approximately represents all stream reaches throughout the CONUS (Mckay et al., 2012). In addition to geographical locations for all stream reaches, each of these 2.67 million stream reaches has additional data associated with it. Specifically relevant to this project, each NHDPlusV2 stream reach has an associated mean discharge in cubic feet per second ("Q0001C"), a length in kilometers ("LengthKM"), and a unitless slope ("SLOPE"). Importantly, these slopes are computed using NED elevations at each end of the reach in conjunction with the length in kilometers of the stream reach (Mckay et al., 2012).

In addition to providing extensive data for each stream reach in the nation, the NHDPlusV2 dataset organizes all stream reaches by hydrologic accounting regions called Hydrologic Unit Codes (HUCs), which are for convenient organization and indexing. These HUCs are widely used in hydrology for organization by different catchments, and this same organization approach is used for the indexing of both the NWM discharge outputs and the HAND database. Consequently, these HUCs were used throughout this analysis in order to enable the use of available NHDPlusV2, NWM, and HAND data. In addition, NHDPlusV2 stream reaches have unique "common identifiers" termed

"COMIDs"; COMIDs will be mentioned throughout this work to refer to specific stream reaches in the NHDPlusV2 dataset.

### 3.2.2 HAND Data

Owing to extensive research, HAND hydraulic properties have been computed for all NHDPlusV2 stream reaches in the CONUS (see Figure 8) (Liu et al., 2017). This research was initially conducted through the National Flood Interoperability Experiment (NFIE), hence the web portal's url location: http://nfie.roger.ncsa.illinois.edu/nfiedata/. These hydraulic properties are organized by 6-digit HUC (HUC-6) regions for convenient organization and ease of use (Seaber, Kapinos, & Knapp, 1987). For all of these regions, in addition to providing a myriad of hydraulic parameters, various datasets are also available, such as DEM raster datasets and shapefiles.

# Index of /nfiedata/HUC6/120902/

| | | |
|---|---|---|
| ../ | | |
| 120902-flows.dbf | 28-May-2016 21:04 | 6540607 |
| 120902-flows.prj | 28-May-2016 21:04 | 165 |
| 120902-flows.shp | 28-May-2016 21:04 | 3410620 |
| 120902-flows.shx | 28-May-2016 21:04 | 29012 |
| 120902-inlets.dbf | 28-May-2016 21:04 | 15893 |
| 120902-inlets.prj | 28-May-2016 21:04 | 165 |
| 120902-inlets.shp | 28-May-2016 21:04 | 37032 |
| 120902-inlets.shx | 28-May-2016 21:04 | 10652 |
| 120902-inlets0.dbf | 28-May-2016 21:04 | 15893 |
| 120902-inlets0.prj | 28-May-2016 21:04 | 165 |
| 120902-inlets0.shp | 28-May-2016 21:04 | 37032 |
| 120902-inlets0.shx | 28-May-2016 21:04 | 10652 |
| 120902-wbd.dbf | 28-May-2016 20:57 | 1121 |
| 120902-wbd.prj | 28-May-2016 20:57 | 165 |
| 120902-wbd.shp | 28-May-2016 20:57 | 115260 |
| 120902-wbd.shx | 28-May-2016 20:57 | 108 |
| 120902-wbdbuf.dbf | 28-May-2016 20:57 | 77 |
| 120902-wbdbuf.prj | 28-May-2016 20:57 | 165 |
| 120902-wbdbuf.shp | 28-May-2016 20:57 | 31740 |
| 120902-wbdbuf.shx | 28-May-2016 20:57 | 108 |
| 120902-weights.tif | 28-May-2016 21:04 | 1171105643 |
| 120902.tif | 28-May-2016 21:04 | 9912580243 |
| 120902_catch.sqlite | 08-Mar-2017 06:07 | 16441344 |
| 120902_comid.txt | 08-Mar-2017 06:07 | 112102 |
| 120902ang.tif | 28-May-2016 21:07 | 1353624702 |
| 120902catchhuc.tif | 03-Jan-2017 20:28 | 19017599 |
| 120902catchmask.tif | 30-Nov-2016 18:26 | 121191738 |
| 120902dd.tif | 28-May-2016 21:10 | 1089416613 |
| 120902fel.tif | 28-May-2016 21:05 | 1354072724 |
| 120902hand.tif | 31-May-2016 01:12 | 1043142099 |
| 120902p.tif | 28-May-2016 21:08 | 106472340 |
| 120902sd8.tif | 28-May-2016 21:08 | 1526197843 |
| 120902slp.tif | 28-May-2016 21:06 | 1535740541 |
| 120902src.tif | 28-May-2016 21:09 | 22062479 |
| 120902ssa.tif | 28-May-2016 21:08 | 37693591 |
| 120902waterbodymask.tif | 06-Jan-2017 18:32 | 5006247 |
| hydroprop-basetable-120902.csv | 08-Mar-2017 06:13 | 31152940 |
| hydroprop-fulltable-120902.csv | 08-Mar-2017 06:13 | 46911305 |
| stderr | 28-May-2016 21:09 | 151761 |
| stdout | 28-May-2016 21:17 | 8513 |

Figure 8: National Flood Interoperability Experiment HAND Data Portal for HUC 6 "120902" (http://nfie.roger.ncsa.illinois.edu/nfiedata/HUC6/120902/).

For this investigation, these HAND rating curve parameters were programmatically retrieved from .csv files containing all HAND data for specific HUC 6 watersheds. As seen in Figure 8, these .csv files were named by HUC-6 code: "hydroprop-fulltable-<HUC6 stream reach identifier>.csv" (ie. hydroprop-fulltable-120902.csv for HUC 120902). Once retrieved, this dataset provides all the information necessary for generating HAND rating

curves for all NHDPlusV2 stream reaches in the CONUS (with an assumed Manning's roughness of 0.05).

### 3.2.3 USGS Data

The USGS publishes an array of hydrologic data collected at their stream gages scattered throughout the country (USGS, n.d.). One particular dataset contains information for rating curves organized by online web address, as shown in Figure 9. These datasets specifically provide streamflow ("INDEP"), stage height ("DEP"), and depth-shift correction ("SHIFT") information. These values are retrieved from frequent field measurements of river cross sections at stream gage locations, coupled with automated surface water depth measurements retrieved by these stream gages.

| INDEP | SHIFT | DEP | STOR |
|---|---|---|---|
| 16N | 16N | 16N | 1S |
| 3.83 | -0.43 | 0.00 | * |
| 3.84 | -0.43 | 0.00 | |
| 3.85 | -0.43 | 0.00 | |
| 3.86 | -0.43 | 0.01 | |
| 3.87 | -0.43 | 0.01 | |
| 3.88 | -0.43 | 0.01 | |
| 3.89 | -0.43 | 0.01 | |
| 3.90 | -0.43 | 0.01 | |
| 3.91 | -0.43 | 0.01 | |
| 3.92 | -0.43 | 0.02 | * |
| 3.93 | -0.43 | 0.02 | |

Figure 9: Representative sample of USGS Water Watch rating curve data for USGS gage 08159000 representing Onion Creek at Highway 183 (https://waterdata.usgs.gov/nwisweb/get_ratings?file_type=exsa&site_no=08159000).

Cross section data are also available through another USGS Water Watch portal containing more detailed information (see Figure 10). Specifically relating to cross sections, this portal provides channel widths ("chan_width"), stage heights

("gage_height_va"), and a data classifier ("current_rating_nu"). From this data, symmetrical cross sections can be approximated that describe the most current USGS field measurements.

| agency_cd | site_no | measurement_nu | measurement_dt | tz_cd | q_meas_used_fg | party_nm | | | | |
|---|---|---|---|---|---|---|---|---|---|---|
| site_visit_coll_agency_cd | | gage_height_va | discharge_va | | current_rating_nu | | shift_adj_va | | | |
| diff_from_rating_pc | | measured_rating_diff | gage_va_change | | gage_va_time | | control_type_cd | | | |
| discharge_cd | chan_nu | chan_name | meas_type | | streamflow_method | | velocity_method | | | |
| chan_discharge | chan_width | | chan_area | | chan_velocity | | chan_stability | | chan_material | |
| chan_evenness | long_vel_desc | | horz_vel_desc | | vert_vel_desc | | chan_loc_cd | | chan_loc_dist | |
| 5s | 15s | 6s | 19d | 12s | 1s | 12s | 5s | 12s | 12s | 4s | 6s | 6s |
| 12s | 7s | 6s | 21s | 15s | 11n | 64s | 4s | 5s | 5s | 14s | 14s | 14s |
| 14s | 4s | 4s | 4s | 12s | 9s | 12s | 7s | 14s | | | | |
| USGS | 08159000 | | 1 | 1924-05-16 | | | Yes | SDB | USGS | 5.52 | 173.0 | |
| 0.00 | | UNSP | 0.00 | | | MEAS | 1 | Unspecified | | UNSP | | |
| 173.0 | | | | UNSP | UNSP | UNSP | UNSP | UNSP | UNSP | UNSP | | |
| USGS | 08159000 | | 2 | 1924-07-15 | | | Yes | SDB | USGS | 4.70 | 18.0 | |
| 0.00 | | UNSP | 0.00 | | | MEAS | 1 | Unspecified | | WADE | QUNSP | |
| 18.0 | 29.0 | 18.0 | 1.00 | UNSP | UNSP | UNSP | UNSP | UNSP | UNSP | UNSP | | |
| USGS | 08159000 | | 3 | 1924-10-08 | | | Yes | M/R | USGS | 3.67 | 3.30 | |
| 0.00 | | UNSP | 0.00 | | | MEAS | 1 | Unspecified | | WADE | QUNSP | |
| 3.30 | 4.50 | 5.30 | 0.620 | UNSP | UNSP | UNSP | UNSP | UNSP | UNSP | UNSP | | |

Figure 10: Representative sample of USGS Water Watch detailed data for USGS gage 08159000 representing Onion Creek at Highway 183 (https://waterdata.usgs.gov/tx/nwis/measurements?site_no=08159000&agency_cd=USGS&format=rdb_expanded)

Importantly, these USGS cross-sections do not include a Gage height at Zero Flow (GZF) value; GZF values were instead shared by Kisters (a large data management firm collaborating with much of the currently ongoing HAND research). Regrettably, GZF values exist only for some USGS gages. Notably, the GZF value is of particular importance because, similar to the bottom-depth shift implemented for all USGS rating curves, a GZF represents the "actual" bottom of a river channel cross-section, rather than the measured bottom on the day the stream was visited. A sample of the GZF values available for Onion Creek are shown in Figure 11 below, showing both the organization of the table as well as the fact that each steam gage may have multiple GZF shifts for each data point.

| AGENCY_C | SITE_NO | STATION_NM | DEC_LAT_V | DEC_LONG_V | GZF_INSP_V |
|---|---|---|---|---|---|
| USGS | 08158700 | Onion Ck nr Driftwood, TX | 30.08298924 | -98.00778589 | 1.46 |
| USGS | 08158700 | Onion Ck nr Driftwood, TX | 30.08298924 | -98.00778589 | 1.52 |
| USGS | 08158700 | Onion Ck nr Driftwood, TX | 30.08298924 | -98.00778589 | 1.74 |
| USGS | 08158827 | Onion Ck at Twin Creeks Rd nr Manchaca, TX | 30.12632345 | -97.82111613 | 4.68 |
| USGS | 08158827 | Onion Ck at Twin Creeks Rd nr Manchaca, TX | 30.12632345 | -97.82111613 | 4.6 |
| USGS | 08158827 | Onion Ck at Twin Creeks Rd nr Manchaca, TX | 30.12632345 | -97.82111613 | 4.52 |
| USGS | 08159000 | Onion Ck at US Hwy 183, Austin, TX | 30.17798987 | -97.68861378 | 4.41 |
| USGS | 08159000 | Onion Ck at US Hwy 183, Austin, TX | 30.17798987 | -97.68861378 | 4.22 |
| USGS | 08159000 | Onion Ck at US Hwy 183, Austin, TX | 30.17798987 | -97.68861378 | 4.14 |
| USGS | 08159000 | Onion Ck at US Hwy 183, Austin, TX | 30.17798987 | -97.68861378 | 4.73 |

Figure 11: Gage height at Zero Flow (GZF) data available for three example stream gages in the Onion Creek watershed. Data received from Kisters.

One final point is important: though using USGS rating curves is a seemingly obvious approach for completing the discharge-to-stage-height conversion, the shortage of USGS rating curve data as compared to the ~2.67 million stream reaches where the NWM is now forecasting discharges is fairly substantial. This extreme shortage of rating curve data must be resolved before this conversion can be reasonably implemented at the national scale. Various approaches to resolving this problem have been undertaken, frequently focusing on model simulations, at-a-station hydraulic geometries, remotely sensed data, etc., though it is unclear if they will integrate appropriately with the new NWM forecasts (Dingman, 2007; Smith & Pavelsky, 2008; Raymond, 2012). This work attempts to address this concern by exploring alternatives to the USGS dataset, hopefully enabling future national-scale rating curve approximations at all 2.67 million stream reaches.

### 3.2.4 HEC-RAS Data

HEC-RAS cross sections along with their associated Manning's roughness values are available from the Austin FloodPro Onion Creek HEC-RAS model (Figure 12) (City of Austin, n.d.). In this visualization, the blue line represents the Onion Creek flowlines, while green lines represents the HEC-RAS cross sections along the stream reaches. Within this HEC-RAS model, all cross sections along the reach are uniquely identified by their so-

called River Station, named in accordance with their distance downstream. Further points laying along the cross section are termed Stations, describing various distances along the cross section with their associated elevation.

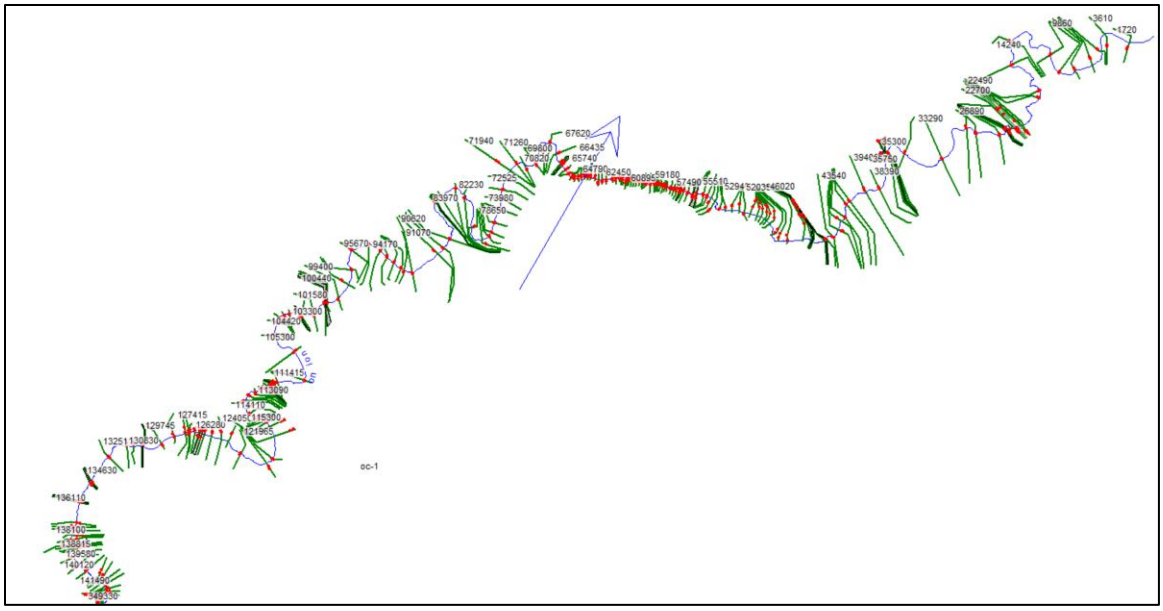

Figure 12: Austin FloodPro HEC-RAS Model for Onion Creek viewed in the HEC-RAS 5.0.3 Desktop Application (City of Austin, n.d.).

An example cross section at River Station 55510 is shown in Figure 13, corresponding to the cross section that is 55,510 feet downstream from the end of this HEC-RAS model stream reach (ie. 0 marks the most downstream end of the reach). This cross section corresponds to the precise location of the USGS stream gage representing Onion Creek at highway 183 in Austin, Texas.

The cross section is represented by the black line, while the black dots along this line represent individual Stations along this cross section. The two red dots denote the divide between the main channel and the over bank channel. Further, the blue "WS" lines and green "EG" lines represent the water surface lines and energy grade lines, respectively.

The black “Ground” line seems to have been added as a representation of bridge piers (to restrict water from entering these areas), which would be consistent with the bridge upon which this gage is placed.

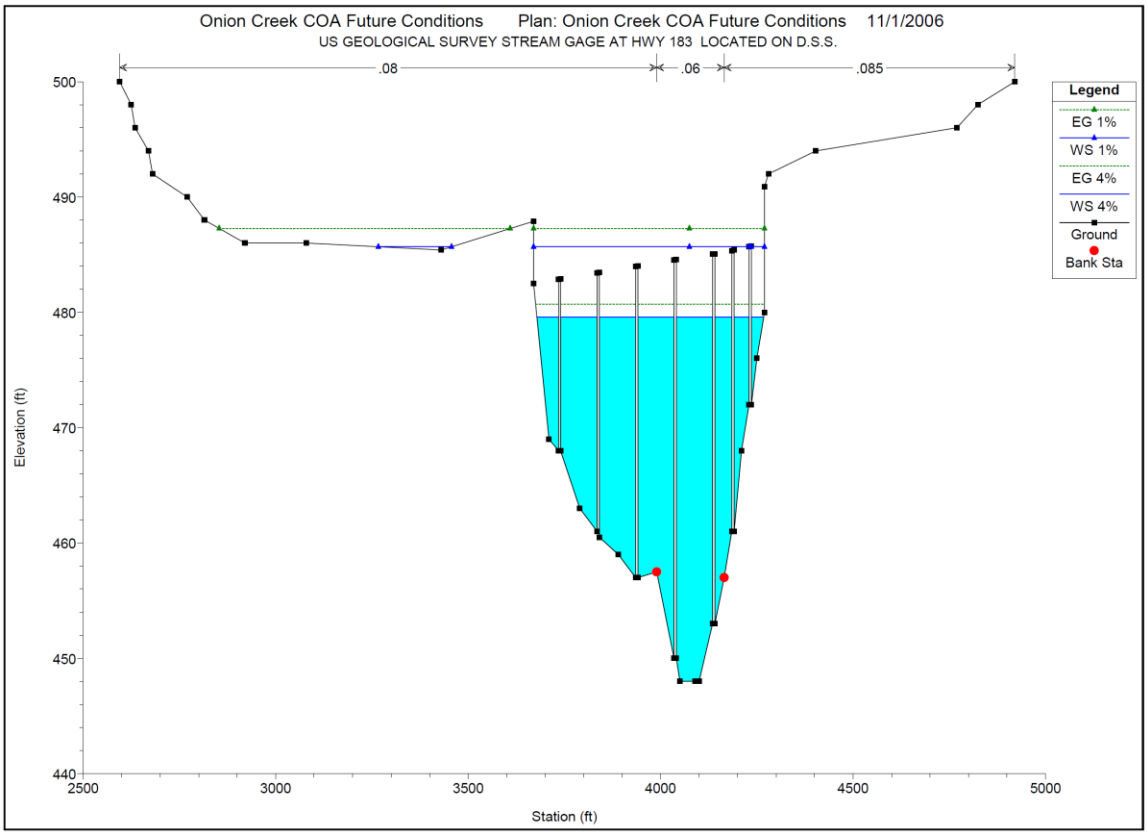


Figure 13: River Station 55510 from Austin FloodPro HEC-RAS Model for Onion Creek viewed in the HEC-RAS 5.0.3 Desktop Application (City of Austin, n.d.).

### 3.3 Preliminary Rating Curve Assessments

Throughout the preliminary study area, HAND, USGS, and HEC-RAS rating curves were constructed for all stream reaches. This rating curve creation is described in the following sections.

### 3.3.1 HAND Rating Curves

HAND rating curves were constructed using Manning's equation. First, $S_0$ was retrieved from the NHDPlusV2 dataset (Mckay et al., 2012). The HAND methodology was then used to determine $A_w$ and $H_R$ for all stream reaches at specified depth intervals (ie. every 1 foot). Rather than re-compute these hydraulic properties, this data was retrieved through the NFIE portal (NFIE, n.d.). Given these hydraulic properties, the only remaining variable required was Manning's roughness coefficient, n.

Manning's roughness can either be retrieved from existing data sources (such as USGS field measurements or HEC-RAS models), or can be determined in the field through observations. Seeing as Manning's roughness values are not currently available for all 2.67 million NHDPlusV2 stream reaches, a Manning's roughness of n = 0.05 was initially assumed. This value was selected simply because it is an average Manning's roughness value, describing a natural stream that is "winding with weeds and pools" (Chow, Maidment, & Mays, 1988). Finally, using all these data, Manning's equation was used to compute discharge for all depth intervals, enabling the generation of synthetic HAND rating curves such as that shown in Figure 14.

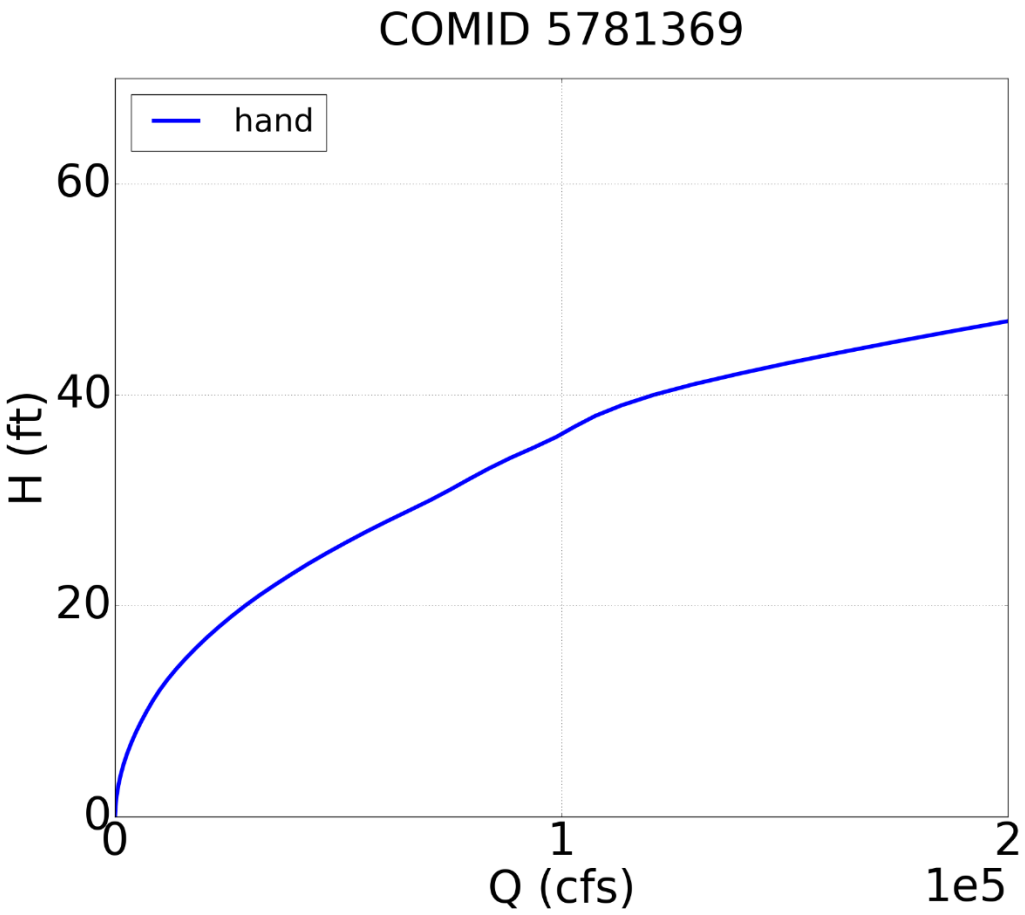


Figure 14: Preliminary HAND rating curve for Onion Creek stream reach COMID 5781369.

By stacking HAND top widths at varying stage heights on top of each other, HAND cross sections can also be created using the HAND methodology (see Figure 15). The two sides of each HAND cross section (centered on the bottom point) are then reflectively symmetric to one another. While this is not precisely representative of a physical channel, this assumption was necessary for this approach to work appropriately. It is important to note that HAND rating curves are unrelated to this methodology and are therefore uncompromised. Additionally, this HAND cross section has not been shifted to correct its geodetic datum; this correction was identified and explored in further sections of the work.

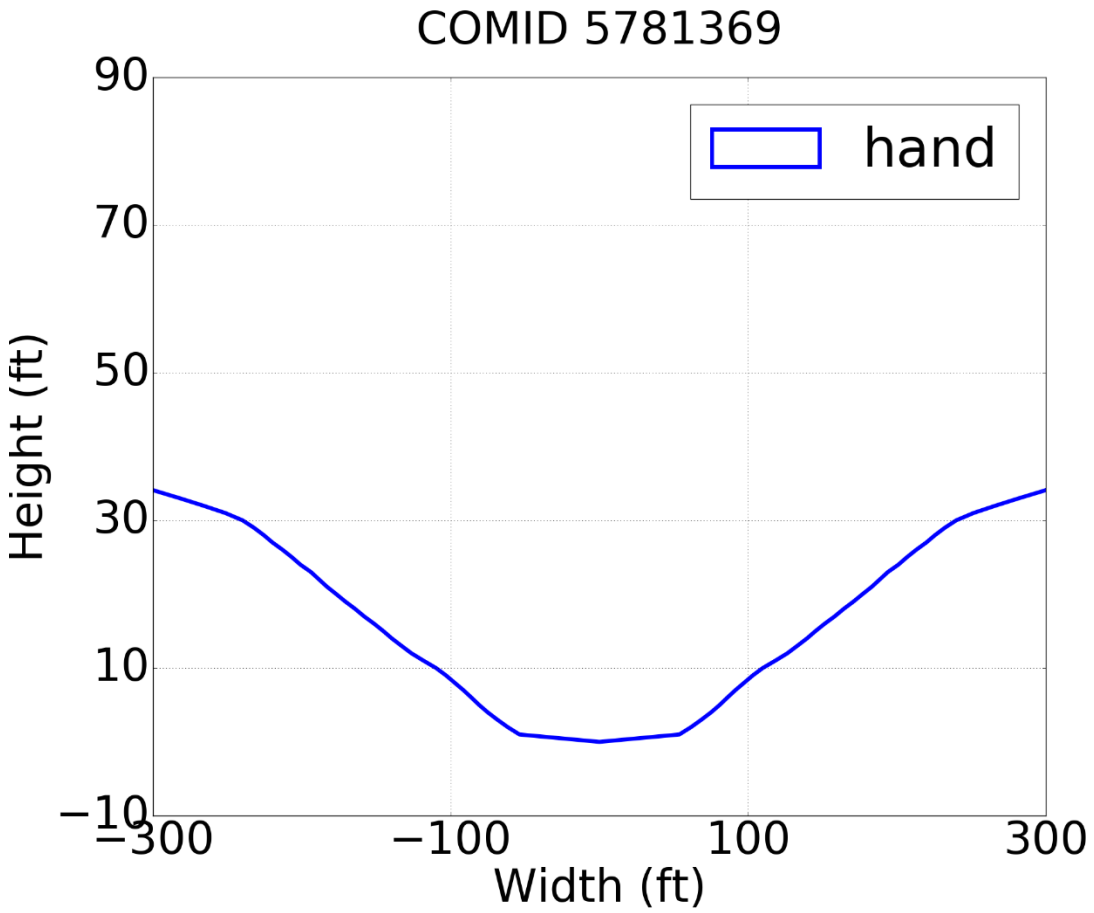


Figure 15: Preliminary HAND cross section for Onion Creek stream reach COMID 5781369.

### 3.3.2 USGS Rating Curves

USGS rating curve data was retrieved by programmatically scraping the USGS online Water Watch database with customized Python scripts. These scripts were written to retrieve stage height, discharge, and depth-shift data before plotting rating curves for visual analysis (see Figure 16). The depth-shift data describes a stage height correction based on USGS field measurements. This depth-shift correction was consequently applied to all USGS rating curves henceforth presented in this research work.

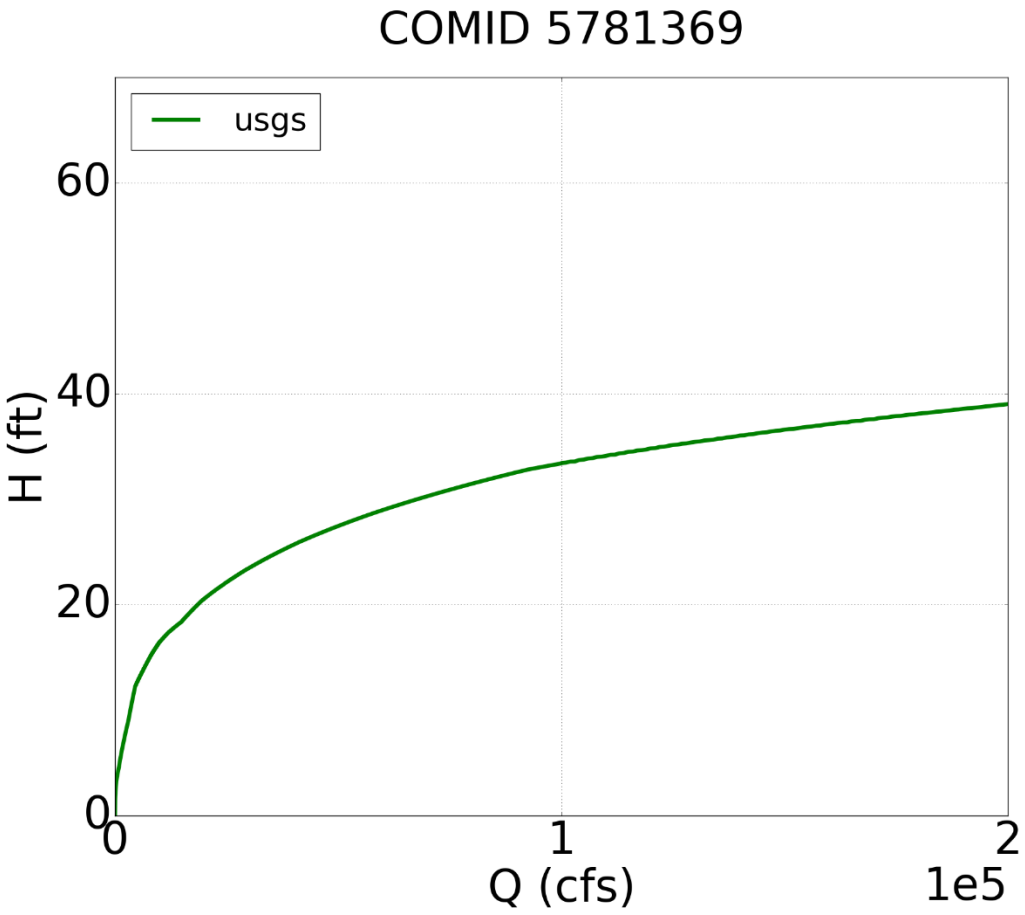


Figure 16: Preliminary USGS rating curve for Onion Creek stream reach COMID 5781369 (USGS gage 08159000).

Identical to the construction of HAND rating curves, USGS channel width data were also available. Channel width information was collected and stacked on top of itself according to the related stage heights, creating another form of reflectively symmetrical cross section (see Figure 17). Importantly, the dataset containing channel width information also included a classifier grouping the data into groups. The USGS changes these groupings whenever a stream reach's hydraulic properties vary significantly, meaning that only the most recent group could be meaningfully compared to the HAND

cross sections. As such, this classifier was used as a selection tool to collect cross section data only for the most recent and up-to-date channel widths available. While this significantly shrinks the dataset, this isolation of only the more recent data was necessary to maintain cross section continuity without including erratic outliers. Notably, this USGS cross section has not been shifted to account for its geodetic datum; this correction was identified and explored in further sections of the work.

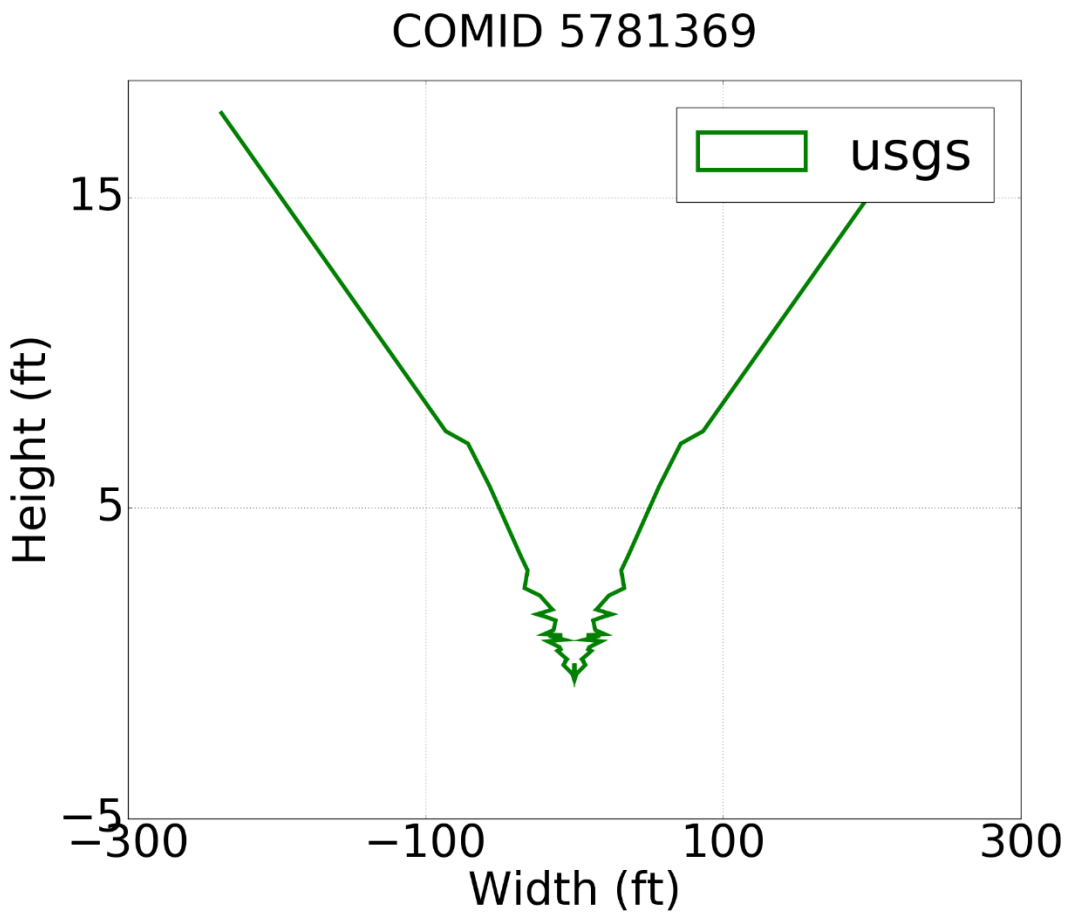


Figure 17: Preliminary USGS cross section for Onion Creek stream reach COMID 5781369 (USGS gage 08159000).

### 3.3.3 HEC-RAS Rating Curves

In the preliminary analysis of HEC-RAS rating curves, information from a previous study compiling Austin FloodPro data and generating rating curves for Onion Creek was used (Zheng, 2015). In this study, HEC-RAS rating curves were created by exporting the available Hydrologic Engineering Center Data Storage System (HEC-DSS) rating curve file, making this data accessible outside of the HEC-RAS model. This process involves reading the HEC-DSS file using a DSS Utility Program (DSSUTL), retrieving the minimum channel elevation of each HEC-RAS cross-section using the HEC-RAS API – HEC-RASController (for VBA integration), locating each cross-section's rating curve using the HEC-RAS River Station nomenclature (detailing the length downstream of each cross-section), and wrapping all this data up together (Zheng, 2015). From this study, a .csv file summarizing HEC-RAS rating curve data for the Onion Creek watershed was available in .csv format (Zheng, 2015).

These HEC-RAS rating curves were then collected and plotted with a Python script (see Figure 18). As in the figure, most NHDPlusV2 catchments have multiple HEC-RAS cross sections within them, resulting in the generation of various HEC-RAS rating curves for each stream reach. Notably, these rating curves are comprised of five hypothetical flood discharges, each representing a point along the rating curve: the 10-year, 25-year, 50-year, 100-year, and 500-year floods. These flood discharges were then plotted as linearly-interpolated lines, consequently resulting in the sharp angle at the front end of the curve (between the origin and the 10-year hypothetical flood discharge).

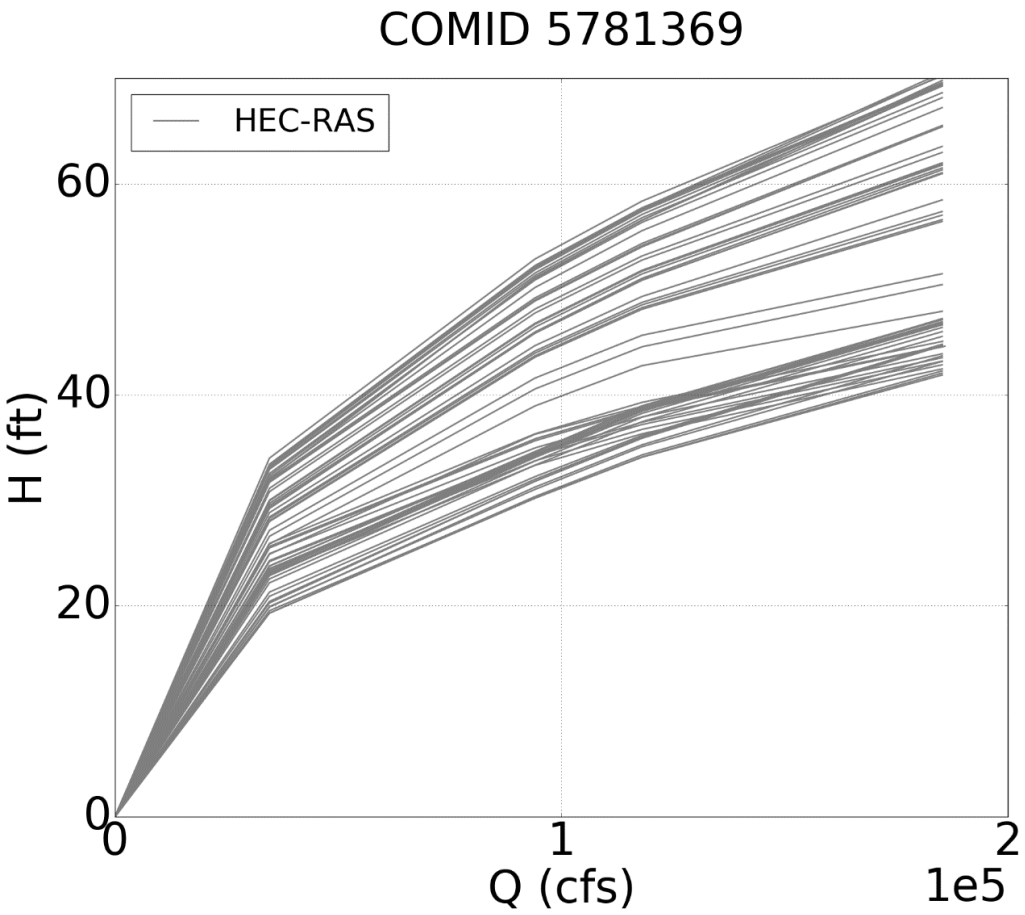


Figure 18: Preliminary HEC-RAS rating curves for Onion Creek stream reach COMID 5781369.

An additional output from this analysis is a shapefile representation of all HEC-RAS cross sections. This output can be viewed and analyzed in ArcGIS or other spatial analysis software, as was shown in Figures 10 through 13.

#### *3.3.3.1 Power-Law Curve Fitting*

Many of the rating curves derived in this work rely on only a few points which must be generalized with a curve fitting. For this curve fitting, a power-law fit was used due to its acceptance in rating curve literature (Reistad, Petersen-Øverleir, & Bogetveit, 2005; Dingman, 2007). Notably, because a power-law function thins out exponentially, marginal

changes in rating curve stage heights eventually become associated with enormous changes in discharge, creating significant under-approximations of stage height moving forward. Despite this complication, a power-law fit generally looks significantly better than a linear regression, and consequently this fitting was used throughout this work. Particularly at lower stage height values, a power-law fit greatly improves the curvature of a rating curve, again justifying its use.

The power-law relationship used in this work is defined by the following equation, where A and B are constants describing the particular rating curve which is being fit:

$$y = Ax^B$$

Power-law curve fitting was accomplished first through a programmatic transformation of all HEC-RAS curves to a natural log – natural log relationship. Following this transformation, a linear fitting of the data was possible, and this fit enabled a computation of the slope (B) and the intercept (logA) of each line. With a bit more manipulation, each HEC-RAS line was successfully fitted with a power-law line, enabling queries on the HEC-RAS dataset at all stage heights.

#### *3.3.3.2 Resistance Function*

In an effort to better understand the large spread of cross-sectional rating curve variation, multiple box-plots were plotted for every stage-height for all reaches in the study area containing HEC-RAS cross-section data. An example of this visual analysis is shown in Figure 19.

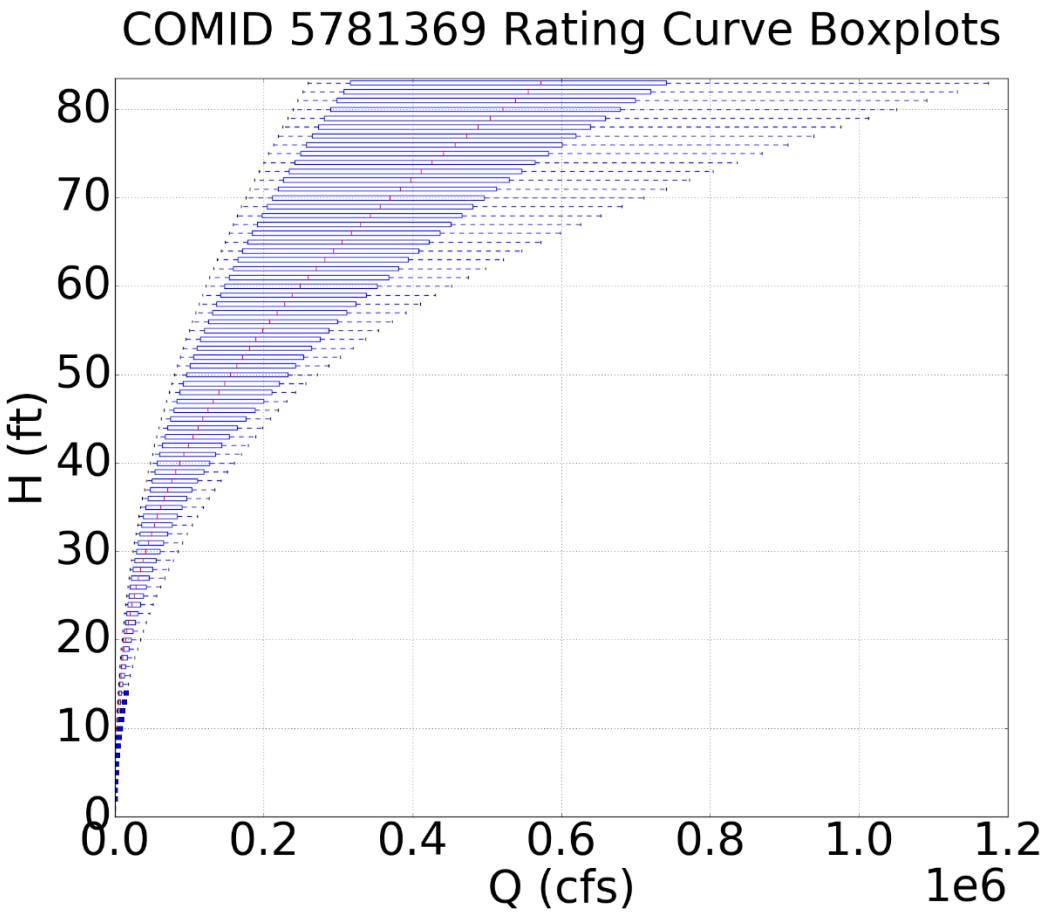


Figure 19: Boxplots denoting the spread of HEC-RAS rating curves for stream reach COMID 5781369.

Following this comparison, HEC-RAS rating curves comparable to the HAND and USGS rating curves were generated using a reach-averaged representation of all HEC-RAS rating curves. This relationship was derived as a "resistance function", so named due to its dependency on variable Manning's roughness coefficients. Importantly, this is not constructed through an averaging of rating curve values at varying stage heights, instead it depends on back-calculated Manning's roughness values at every stage height.

To construct the resistance functions for each catchment, a Manning's roughness value was back-calculated for each stage height between 0 and 82 feet (this extent of stage

heights was chosen for consistency with the HAND rating curve stage height data). This back-calculation relied on NHDPlusV2 slope values as well as HAND wetted area and hydraulic radius values. Using this information and the discharge (retrieved by reading each HEC-RAS rating curve for the stage height in question), a Manning's roughness was computed for each HEC-RAS curve at that particular stage height. Once all of these Manning's roughness values were computed, all these roughness values within a stream reach could be averaged together by stage-height (ie. one roughness average for every 1-foot stage height interval), and a single representative rating curve, the "resistance function", could be created describing the entire reach (see Figure 20).

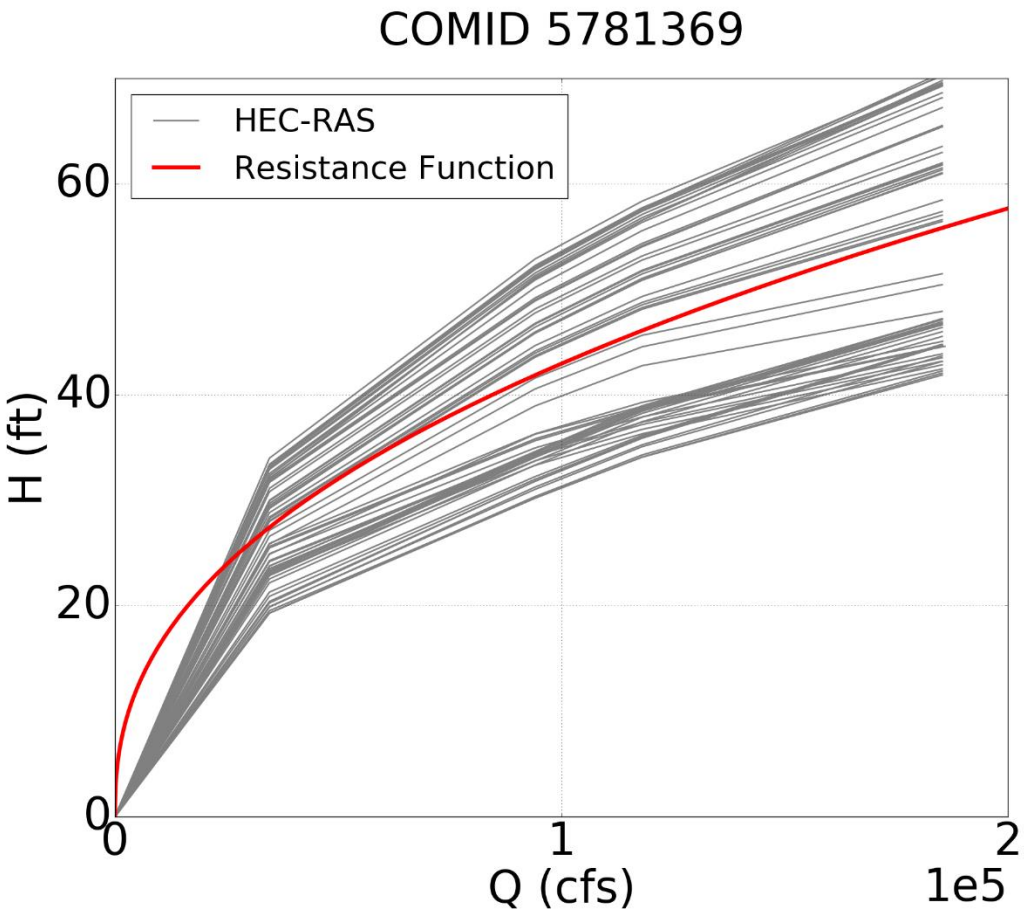


Figure 20: Preliminary HEC-RAS rating curves for Onion Creek stream reach COMID 5781369 (in grey) with "resistance function" (in red).

### 3.4 Preliminary Cross Section Assessments

In addition to rating curve analyses, cross sections were also explored as a potentially useful metric for assessing the performance of the HAND methodology. This comparison was only conducted between HAND and USGS cross sections in avoidance of the monstrous variations of the HEC-RAS cross sections.

#### 3.4.1 HAND Cross Sections

HAND cross sections were created using the channel width and stage height data available through the NFIE web portal. A Python script was written to iterate through all

stage heights and channel widths, consequently stacking them up on top of each other in a typical cross sectional plot. These cross sections were then positioned at the appropriate elevation using geodetic datum elevations retrieved using ArcGIS.

Seeing as a HAND cross-section is representative of a whole reach, the geodetic datum was collected at the USGS gage location from the 10-meter NED upon which HAND is generated. This was done for consistency when comparing with the USGS location which (ideally) would have a similar geodetic datum value. In order to collect this geodetic datum value, the USGS gages first had to be snapped to their nearest NHDPlusV2 streamline using the ArcGIS "snap" tool. Following this spatial adjustment, the 10-meter NED was read at each USGS gage in question using the ArcGIS "Extract Multi Values to Points" tool, resulting in a table containing COMIDs and 10-meter NED elevations. These elevations were treated as the representative geodetic datum of the HAND cross sections, depending on the COMID of the HAND stream reach. An example HAND cross section constructed in this way is shown in Figure 15.

### 3.4.2 USGS Cross Sections

Constructed similarly to the HAND cross sections, USGS cross sections relied on width and depth data, with an additional depth shift step required. This depth shift was collected from the GZF values corresponding to these USGS stream gages, though notably only the most recent GZF value was used for each stream gage, rather than an average of all previously observed GZF values together. Additionally, not all USGS stream gages in the Onion Creek watershed contained GZF adjustments, thereby nullifying the relevance of any HAND and USGS cross section comparisons for these stream reaches.

Once USGS cross sections were collected and properly tweaked according to any GZF data available, the geodetic datum describing the elevation above sea level was

retrieved for each cross-section. The geodetic datum information for all USGS gaging stations is available on each cross-section's Water Watch webpage (USGS, n.d.); this data was scraped from the web for all COMIDs in question using another Python script.

Specifically for the USGS gages, a particular spatial reference of the datum was retrieved as well, as some gages were listed using the National Geodetic Vertical Datum of 1929 (NGVD 29) while others used the North American Vertical Datum of 1988 (NAVD 88). Importantly, these two reference systems are similar but different, meaning that in a more complex study a conversion may be necessary to precisely retrieve USGS elevations. In this fundamental assessment this conversion was ignored, seeing as the conversion would likely create errors of up to only a few feet (FEMA, 2013). This was acceptable for the visual comparisons made in this work. An example USGS cross section constructed using this methodology is shown in Figure 17.

### 3.5 Revised Study Area

Over the course of this study, it became apparent that analysis at the river level would be more informative than at the watershed level. After realizing this, the study area was adjusted to reflect a new focus on Onion Creek as a river rather than the entire watershed. As shown in Figure 21, local USGS gages are represented by the red "OnionCk_StreamGages" circles, HEC-RAS cross sections are represented by purple "OnionCk_XSects" lines, and NHDPlusV2 stream reaches are represented by blue lines sized according to their mean annual flowrate ("Q0001C"). This change was made primarily for two reasons. First-off, the initial reasoning for studying Onion Creek as a sample set of various catchments throughout the Onion Creek area was due to the availability of USGS data; this USGS data was later determined to be less useful than the HEC-RAS data for this analysis, so this benefit was no longer relevant. The second reason

is that observation across a continuous stream reach enabled more thorough analysis not only of roughness values and slopes (which both affect rating curves), but also of the way these parameters change along the stream reach as one larger entity. These analyses were considered to be critical for the overall generalization of the HAND methodology on a larger scale, and therefore this shift in study area was necessary.

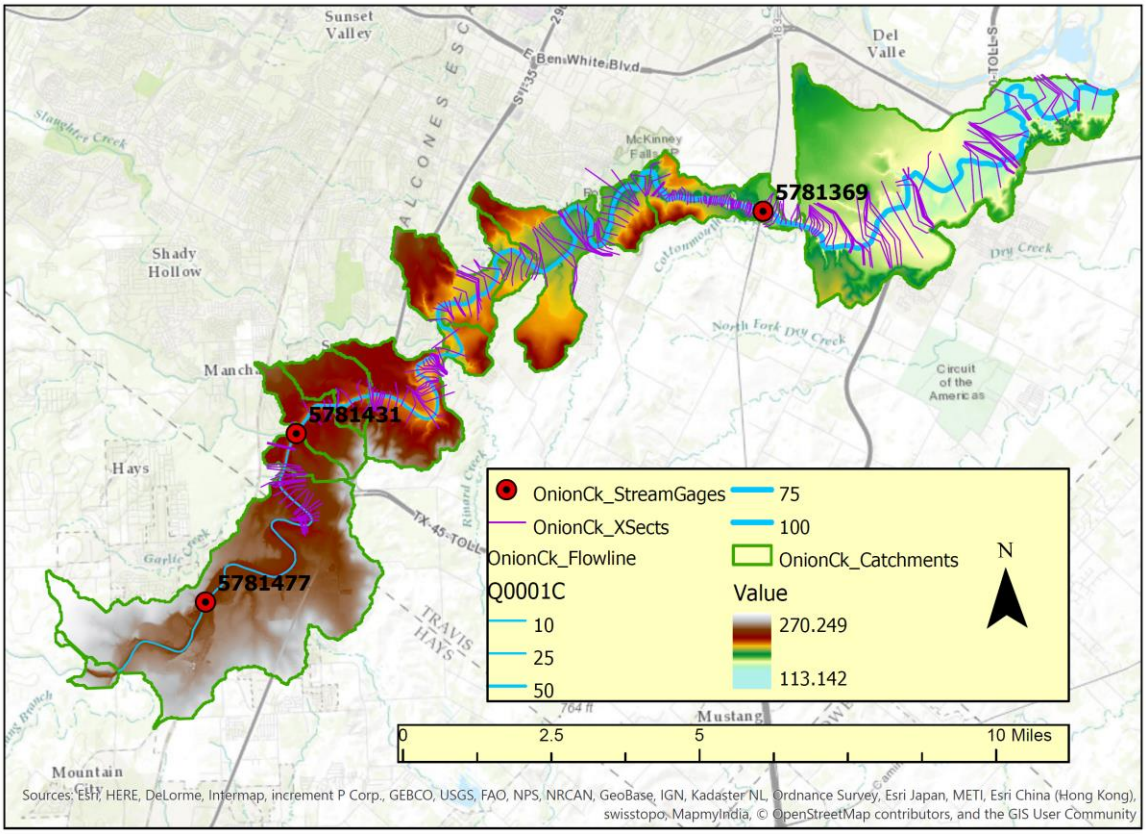


Figure 21: Revised study area representing only Onion Creek rather than the entire Onion Creek watershed.

As shown in Figure 21, HEC-RAS cross section data are available for the entirety of Onion Creek, while USGS gaging stations are only available at three locations (one of which contains no useful HEC-RAS data for comparison, so truly data for only two USGS

gages is useful). Due to this relative scarcity of USGS data, comparison between HAND and HEC-RAS rating curves became the focus of analysis moving forward.

### 3.6 Stream Profile

Once the study area was revised, the next step in comparing HAND and HEC-RAS data was to recognize that HAND is generated using the NED DEM. As such, any differences between the NED and the elevations used in the Onion Creek HEC-RAS model would be informative. Consequently, the next study involved a stream profile comparison between the HAND and HEC-RAS stream profiles. USGS data was not included due to the relative scarcity of information along Onion Creek; any attempt to create a stream profile would have had only two or three points along Onion Creek, resulting in an uninformative stream profile.

For this comparison, only the minimum elevation value is needed from the HEC-RAS dataset, and thus all other cross-section Stations were removed. The results of this generalization were arrived at by relating each RiverStation only to its lowest Station's elevation value (see Figure 22, where "RAS" is the column denoting the HEC-RAS lowest elevation values).

| RiverStati | RAS |
|---|---|
| 100220 | 525 |
| 100300 | 525 |
| 100350 | 525 |
| 100400 | 525 |
| 100440 | 525 |
| 101580 | 526.6 |
| 102450 | 528.5 |
| 102500 | 528.5 |
| 102600 | 528.5 |
| 102650 | 528.5 |
| 103300 | 530.8 |
| 103675 | 531.5 |

Figure 22: Sample of River Stations for cross sections along Onion Creek with their associated minimum HEC-RAS elevations.

After simplifying the HEC-RAS data, minimum DEM elevations were retrieved for each HAND stream reach using a raw DEM ("120902.tif"), a filled DEM ("120902.fel"), and DEM-derived flowlines ("120902.src") (NFIE, n.d.). All these data were specified by HUC-6, similar to all other HAND data organization seen previously in Figure 8. The raw DEM is simply a normal DEM, the filled DEM has all pits removed, and the DEM-derived flowlines are the equivalent of the NHDPlusV2 flowlines except that they are derived from the DEM (and consequently differ slightly). Before processing, only the DEM-derived flowlines intersecting the Onion Creek cross sections were selected and exported to a new shapefile.

Using these datasets along with a shapefile of the HEC-RAS cross sections, a customized ArcGIS script was used to extract the values of the filled and unfilled DEMs where each HEC-RAS cross section intersects with the DEM-derived flowlines. The results

of this data extraction are shown in Figure 23, displaying each River Station along with its DEM and FEL (filled DEM) values (in feet).

| XCoord | YCoord | RIVER | REACH | RIVSTATIC | DEM_FT | FEL_FT |
|---|---|---|---|---|---|---|
| -97.72 | 30.18841 | onion | oc-1 | 67620 | 476.6102 | 478.2766 |
| -97.7188 | 30.18637 | onion | oc-1 | 66435 | 468.1923 | 468.1923 |
| -97.7178 | 30.18463 | onion | oc-1 | 65740 | 466.7366 | 466.7366 |
| -97.7176 | 30.18445 | onion | oc-1 | 65690 | 466.856 | 466.856 |
| -97.7175 | 30.18429 | onion | oc-1 | 65620 | 466.2143 | 466.2143 |
| -97.7175 | 30.18427 | onion | oc-1 | 65580 | 466.2143 | 466.2143 |
| -97.7168 | 30.1834 | onion | oc-1 | 65170 | 464.7563 | 465.0241 |
| -97.7161 | 30.18258 | onion | oc-1 | 64790 | 464.2668 | 464.2668 |
| -97.7155 | 30.18204 | onion | oc-1 | 64540 | 463.2075 | 463.2075 |
| -97.7149 | 30.18177 | onion | oc-1 | 64305 | 462.8154 | 462.8154 |
| -97.714 | 30.18184 | onion | oc-1 | 63985 | 461.9182 | 461.9182 |

Figure 23: Sample of River Stations and associated unfilled (DEM) and filled (FEL) DEM values extracted from the NED.

These values were then combined with the HEC-RAS minimum elevations (Figure 22) and plotted as a stream profile for comparison. The result of this comparison for Onion Creek is shown in Figure 24, displaying the minimum elevation differences between HAND (represented by DEM and FEL) and the HEC-RAS model. The DEM-based stream profiles vary significantly more than the HEC-RAS stream profile, resulting in more slope variability throughout the stream reach. This has problematic implications on slope which will be explored later.

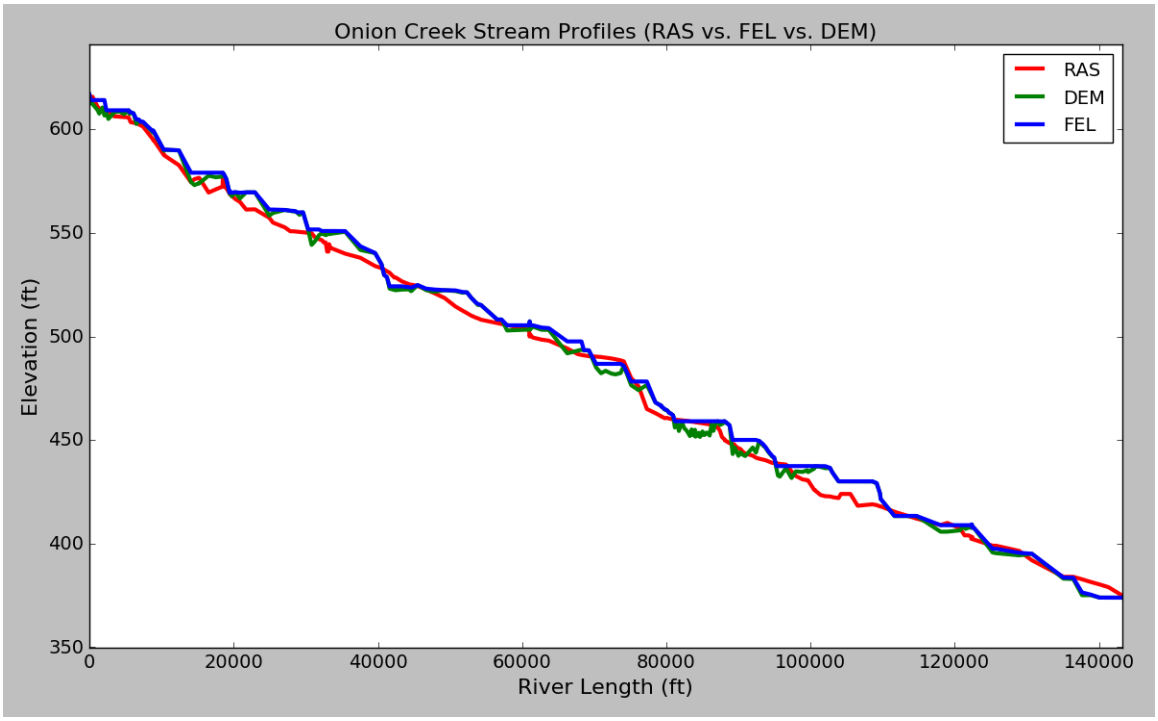


Figure 24: Stream profile showing HAND (DEM and FEL) and HEC-RAS (RAS) elevations along the entire length of Onion Creek.

### 3.7 Detailed Rating Curve Assessments

As this research progressed, the focus shifted from locating individual HEC-RAS cross-sections for each stream reach to become a more thorough analysis using reach-averaged median HEC-RAS rating curves (this is different from the above-described resistance function curves). These reach-averaged HEC-RAS rating curves were then methodically compared to HAND rating curves to resolve any differences. Additionally, the study area revisions enable the entirety of Onion Creek to be assessed, searching for generalizable trends in HEC-RAS rating curve differences as compared to HAND rating curves. These generalizable differences are the real question, with the true objective being the elimination of HAND inconsistencies on a national scale.

### 3.7.1 Revised HEC-RAS Rating Curves

Using a Python script, Onion Creek cross section data was extracted from the HEC-RAS model. The results of this extraction are a .csv output summarizing the data at all points on the HEC-RAS cross section, specifically capturing each point's Station and Elevation as shown in Figure 25. The Station value describes how far along the cross section each point is (in feet, following the cross section's length), and the Elevation is simply the elevation of each of these Stations (also in feet).

| River | Reach | RiverStati | Station | Elevation | Source |
|---|---|---|---|---|---|
| onion | oc-1 | 349330 | 1000 | 1168.9 | Onion_OnionCr_g01 |
| onion | oc-1 | 349330 | 1008 | 1167.7 | Onion_OnionCr_g01 |
| onion | oc-1 | 349330 | 1095 | 1161.8 | Onion_OnionCr_g01 |
| onion | oc-1 | 349330 | 1196 | 1157 | Onion_OnionCr_g01 |
| onion | oc-1 | 349330 | 1297 | 1153.7 | Onion_OnionCr_g01 |
| onion | oc-1 | 349330 | 1381 | 1150.7 | Onion_OnionCr_g01 |
| onion | oc-1 | 349330 | 1383 | 1148 | Onion_OnionCr_g01 |
| onion | oc-1 | 349330 | 1416 | 1151 | Onion_OnionCr_g01 |
| onion | oc-1 | 349330 | 1497 | 1153.6 | Onion_OnionCr_g01 |

Figure 25: Sample of Onion Creek HEC-RAS cross section data extracted from the model and summarized in .csv format.

Using this information, HEC-RAS rating curves for various discharge values were created for all HEC-RAS cross sections. To generate these rating curves, various discharge values were first collected for each stream reach before they could be run through the HEC-RAS model. From the NHDPlusV2 dataset, mean annual discharge was collected for all locations where HEC-RAS River Stations and NHDPlusV2 flowlines intersect. A sample of this data after it was extracted is shown in Figure 26, representing each river station and the mean annual flow for the NHDPlusV2 stream reach it intersects (denoted by the "Q0001C" column).

| XCoord | YCoord | RIVER | REACH | RIVSTATIC | COMID | Q0001C |
|---|---|---|---|---|---|---|
| -97.6771 | 30.17415 | onion | oc-1 | 50750 | 5781385 | 71.804 |
| -97.6756 | 30.17368 | onion | oc-1 | 50240 | 5781385 | 71.804 |
| -97.6749 | 30.17337 | onion | oc-1 | 49960 | 5781385 | 71.804 |
| -97.6742 | 30.17301 | onion | oc-1 | 49660 | 5781385 | 71.804 |
| -97.6736 | 30.1727 | onion | oc-1 | 49440 | 5781385 | 71.804 |
| -97.673 | 30.17231 | onion | oc-1 | 49190 | 5781385 | 71.804 |
| -97.6721 | 30.17037 | onion | oc-1 | 48340 | 5781385 | 71.804 |
| -97.6691 | 30.16885 | onion | oc-1 | 46980 | 5781385 | 71.804 |
| -97.6657 | 30.16924 | onion | oc-1 | 46020 | 5781385 | 71.804 |
| -97.6639 | 30.16898 | onion | oc-1 | 45400 | 5781385 | 71.804 |

Figure 26: Sample of Onion Creek HEC-RAS River Stations and associated NHDPlusV2 mean annual discharge ("Q0001C").

These mean annual flow data were then simplified by removing any duplicated COMIDs. This was done by selecting only the most upstream River Station in each COMID, and removing all other River Stations that share the same COMID value. Logically this is acceptable because the NHDPlusV2 mean annual discharge values are unique only at the stream reach scale, meaning that, as seen in Figure 26 above, these mean annual discharges are identical for all River Stations with the same COMID. This removal of downstream River Stations therefore did not impact the HEC-RAS model results.

#### *3.7.1.1 USGS 100-year Flood Regression*

Following the collection of this data, a 100-year flood regression was computed using a flood regression methodology derived by the USGS (Asquith & Roussel, 2009). This flood regression methodology is based on the following equation:

$$Q_{100} = P^{1.071} S^{0.507} 10^{[0.969\Omega + 10.82 - 8.448A^{-0.0467}]}$$

Where $Q_{100}$ represents the 100-year discharge, P represents mean annual precipitation (inches), S is the main-channel slope, Ω is a generalized terrain and climate index, and A represents the drainage area (square miles).

Using this equation, a 100-year flood discharge was computed for all catchments along Onion Creek. Annual precipitation draining to each stream reach, channel slope of each stream reach, and drainage area to each stream reach were all retrieved from the NHDPlusV2 dataset as "P_inch", "SLOPE", and "TotDASqMI", respectively. The OMEGA value was retrieved from Figure 26, retrieved from the USGS work in which the equation was derived (Asquith & Roussel, 2009). According to Figure 27, the OMEGA value for all of Onion Creek is 0.125. Figure 28 shows an example of this calculated 100-year flood discharge for COMID 5781939 using the stream reach's local NHDPlusV2 properties and the Onion Creek OMEGA value of 0.125.

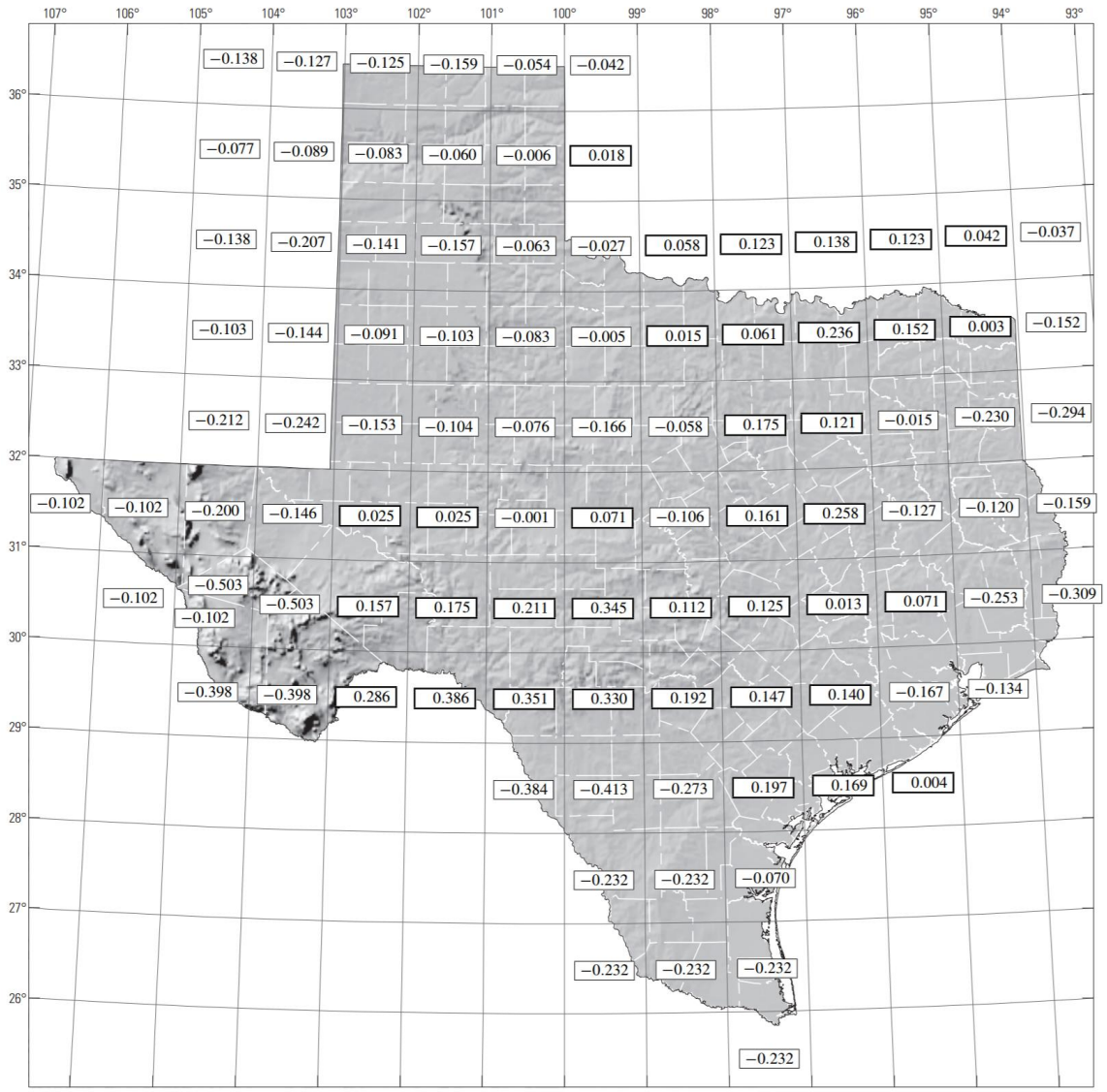


Figure 27: Omega parameter representing a generalized terrain and climate index for Texas (Asquith & Roussel, 2009).

| COMID | SLOPE | Q0001C_cfs | TotDASqMl | P_inch | Omega | Q100_c | |
|---|---|---|---|---|---|---|---|
| 5781939 | 0.00001 | 52.57 | 233.776001 | 35.0795 | 0.125 | 3254.927 | 61.91606 |

Figure 28: Example of calculated 100-year flood discharge for COMID 5781939.

#### *3.7.1.2 Slope Assumption*

Before continuing with the analysis, the flood regression 100-year flood discharge was compared to the HEC-RAS 100-year flood discharge (retrievable from the HEC-RAS model) for each stream reach. In the case of Onion Creek, these values differed significantly, and as such the slope was modified to approach a more reasonable 100-year discharge. Initially this shift was made by using a calculated average slope of all Texas stream reaches (0.00623), but this slope still resulted in a significant error and was therefore not as useful as anticipated.

Finally, the optimal slope for creating a minimal difference between the HEC-RAS and HAND 100-year floods curves was computed for Onion Creek as 0.00999, and the flood-regression slope was manually changed to this value. After this change, both 100-year flood values matched much better, and the analysis could continue. It is very important to note that this was initially considered an unreasonable approach. However, after careful assessment, it was ultimately determined that the intent of this research is to improve the relationship between discharge and stage height (ie. rating curves), and as such determining the correct discharge was not within this scope. This is particularly true seeing as discharges from the NWM will ultimately be used for any real-time flood forecasting. Consequently, this manipulated discharge value was used to match HEC-RAS 100-year flood discharges as closely as possible while still remaining consistent in its derivation method using the USGS equation introduced above.

#### *3.7.1.3 Final HEC-RAS Rating Curves*

After correcting these discharge assumptions, a series of eight linearly-interpolated discharge values were generated between the mean annual flow (“Q0001C” from NHDPlusV2) and the 100-year flood discharge (100-year flood regression discharge using a manually corrected slope). Eight values were selected as a good balance to maintain

model efficiency while simultaneously providing sufficient data to generate meaningful HEC-RAS rating curves (Figure 29). The important difference to note here is the increase in water surface lines (blue lines) as compared to Figure 13.

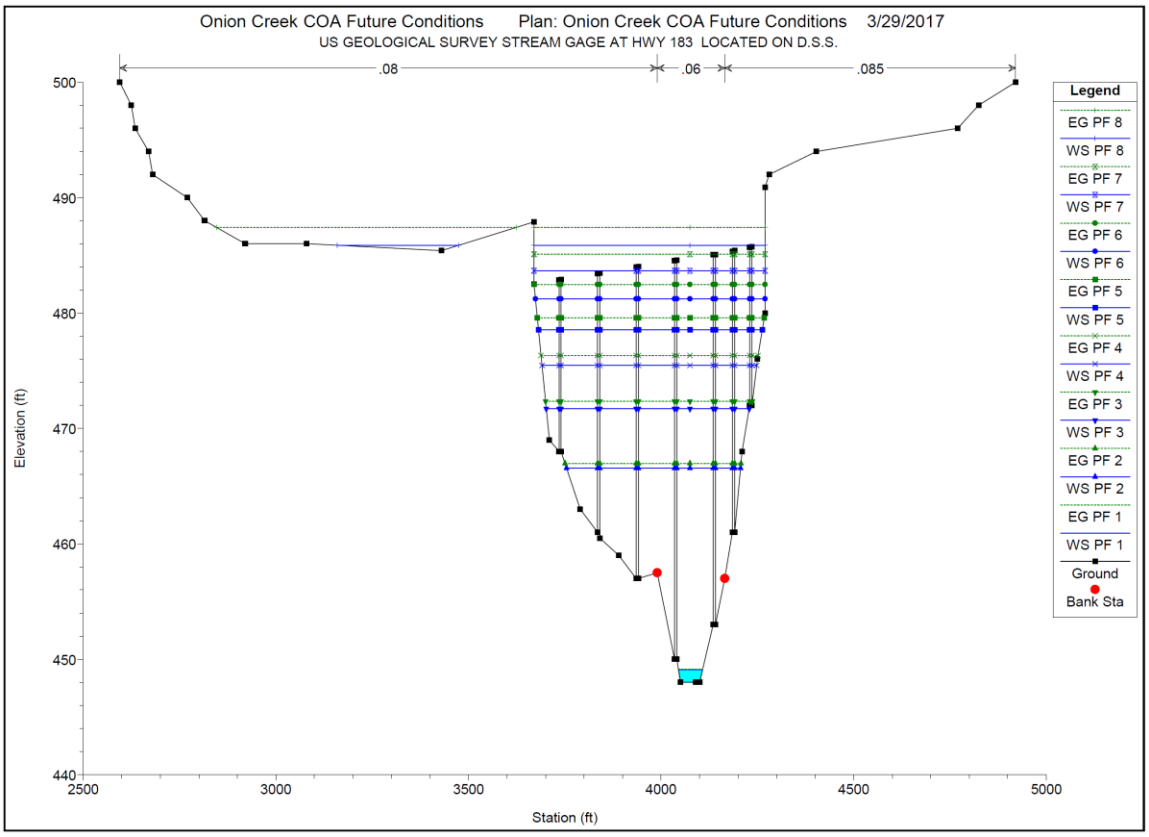


Figure 29: HEC-RAS cross section for River Station 55510 with eight stage heights corresponding to the eight discharges linearly interpolated between the stream reach's mean annual discharge and 100-year flood regression.

Using these eight linearly-interpolated discharge values and running the HEC-RAS model, eight stage height results were generated, one for every discharge value. This ultimately enabled the generation of a rating curve from these various discharge/stage-height data pairs, which were again extracted programmatically. An example of a resulting rating curve is shown in Figure 30.

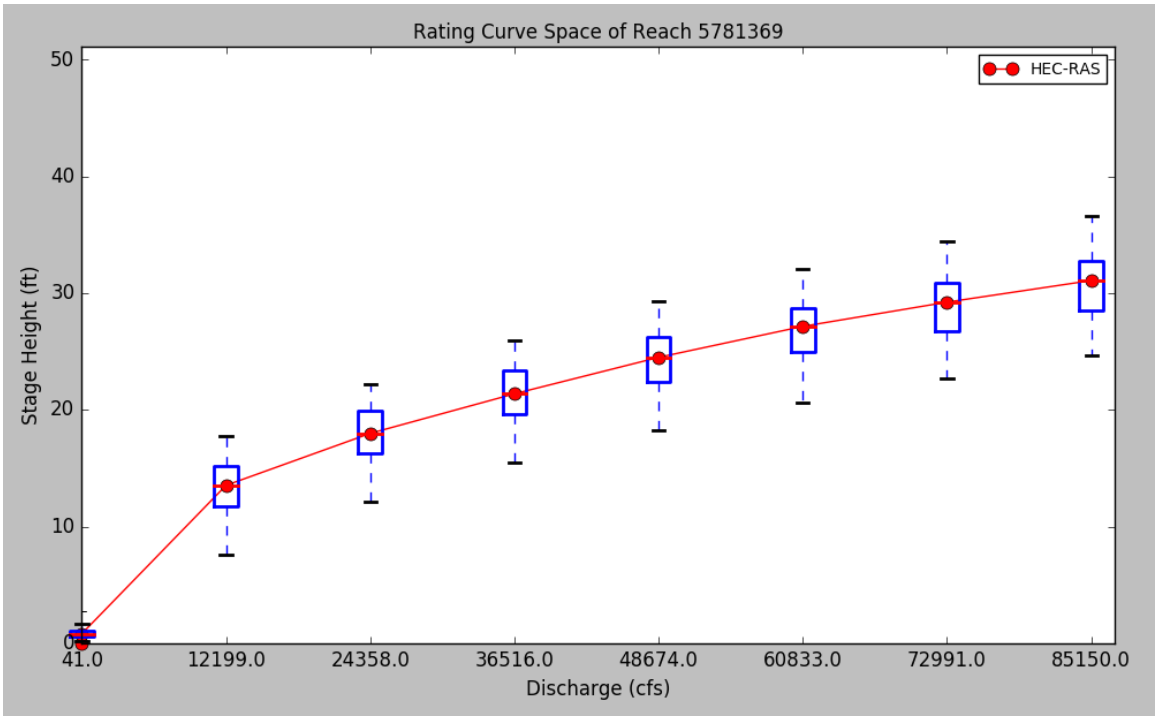


Figure 30: HEC-RAS median rating curve for COMID 5781369, with box plots representing the spread of all HEC-RAS curves within this COMID.

### 3.7.2 HAND vs. HEC-RAS

Using the current HAND assumption of Manning's roughness equal to 0.05, a preliminary look at the differences of HAND and HEC-RAS can be observed. An initial look at this (see Figure 30) shows that, though there are differences between the blue HAND curve and the red HEC-RAS curve, the 0.05 assumption seems to perform quite well for this particular stream reach. This form of visual comparison will be revisited in the results section, exploring alternative HAND rating curves and their performance.

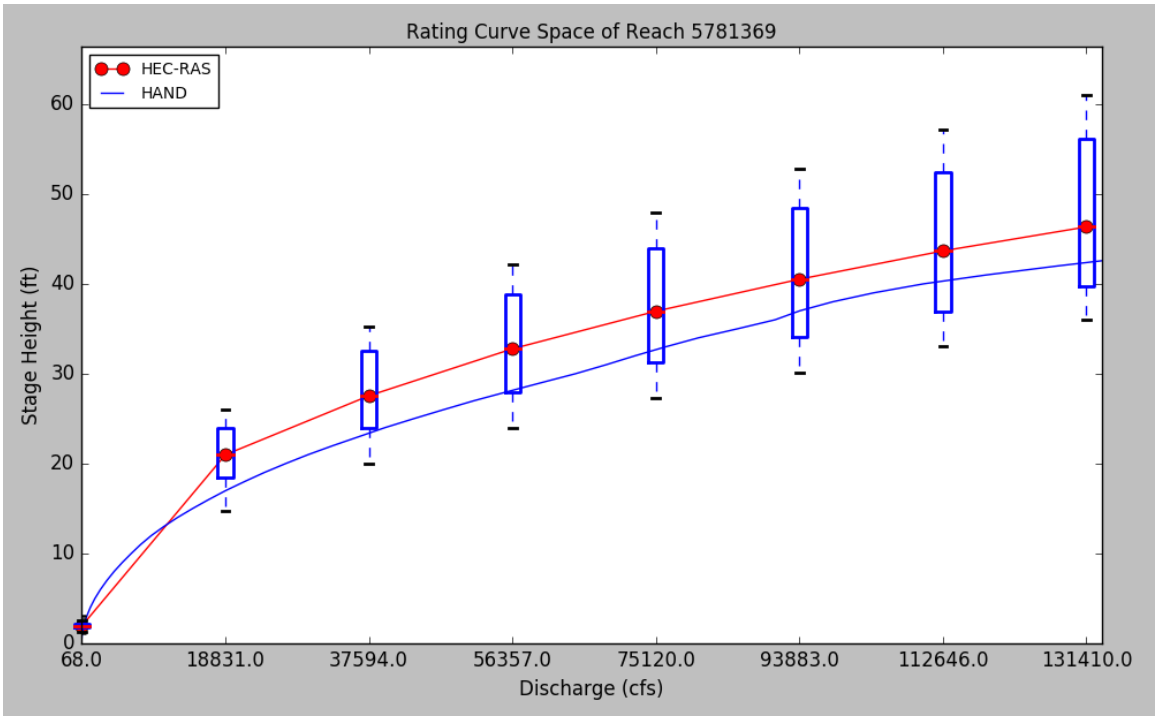


Figure 31: Original HAND rating curve (with Manning's roughness assumption of 0.05 and NHDPlusV2 slope) as compared to the HEC-RAS rating curve for the same reach, COMID 5781369.

## 3.8 Potential Improvements

The following sections present investigations in improving the current HAND rating curve to more closely match the stream reach-averaged HEC-RAS rating curves, both shown in Figure 31.

### 3.8.1 Rating Curve Depth-Shift

The first potential solution investigated was intended to address the false bottom created by using DEM-derived HAND rating curves. Despite recent technological improvements (Hernandez & Armstrong, 2016), DEMs often have problems sensing river bathymetry due to failings to penetrate surface water. This shortcoming often leads to DEM-based river elevations being higher, resulting in larger stream widths due to cut-off

channel bottoms, and ultimately decreasing stage heights. This could easily be a reason for the HAND curve being lower than the HEC-RAS curve in Figure 30.

In resolving this issue, the HEC-RAS cross-sections were used as a guide by retrieving the HEC-RAS depth at zero discharge. This depth was determined by finding the width of the river reach at a HAND depth of zero feet (width is determined by summing the number of pixels along the transverse axis to the reach). A corresponding discharge is then read off of the median HEC-RAS rating curve, resulting in a discharge shift. Once these values were determined, the HAND rating curve was adjusted to reflect the physical depth captured by the HEC-RAS rating curve (which is assumedly missed by the HAND rating curve). Similarly, a shift in discharge was also applied to account for the discharge that would exist in this false bottom if it was accounted for. After this analysis, the HAND rating curves were generally shifted up, beginning at a positive depth and discharge (rather than at the origin), as shown in Figure 32.

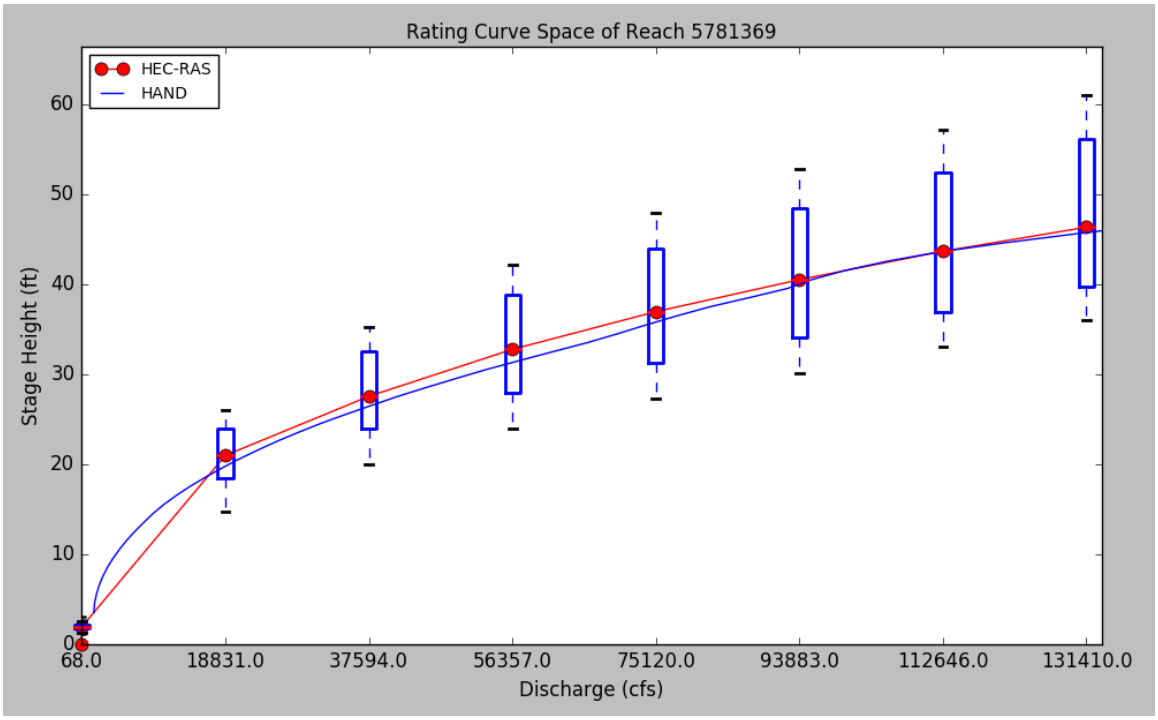


Figure 32: HAND rating curve with a depth shift applied (with Manning's roughness assumption of 0.05 and NHDPlusV2 slope) as compared to the HEC-RAS rating curve for the same reach, COMID 5781369.

### 3.8.2 Manning's Roughness Edits

In an effort to further improve the fit of the HAND rating curves, edits to the 0.05 roughness assumption were explored next.

#### *3.8.2.1 NLCD Catchment Averaged Roughness*

Attempting to intelligently determine Manning's roughness for all stream reaches in the CONUS, roughness relationships between Manning's roughness and the 2011 National Land Cover Database (NLCD) (Homer et al., 2015) were sought out. Luckily, an informative review summarized and generalized previous findings to relate a Manning's roughness value to all NLCD classifications as follows (Figure 33) (Moore, 2011).

| NLCD Classification | Manning's n | | | Source |
|---|---|---|---|---|
| | Minimum | Normal | Maximum | |
| Open Water | 0.025 | 0.03 | 0.033 | Chow 1959 |
| Developed, Open Space | 0.01 | 0.013 | 0.016 | Calenda, et al. 2005 |
| Developed, Low Intensity | 0.038 | 0.05 | 0.063 | Calenda, et al. 2005 |
| Developed, Medium Intensity | 0.056 | 0.075 | 0.094 | Calenda, et al. 2005 |
| Developed, High Intensity | 0.075 | 0.1 | 0.125 | Calenda, et al. 2005 |
| Barren Land | 0.025 | 0.03 | 0.035 | Chow 1959 |
| Deciduous Forest | 0.1 | 0.12 | 0.16 | Chow 1959 |
| Evergreen Forest | 0.1 | 0.12 | 0.16 | Chow 1959 |
| Mixed Forest | 0.1 | 0.12 | 0.16 | Chow 1959 |
| Scrub/Shrub | 0.035 | 0.05 | 0.07 | Chow 1959 |
| Grassland/Herbaceous | 0.025 | 0.03 | 0.035 | Chow 1959 |
| Pasture/Hay | 0.03 | 0.04 | 0.05 | Chow 1959 |
| Cultivated Crops | 0.025 | 0.035 | 0.045 | Chow 1959 |
| Woody Wetlands | 0.08 | 0.1 | 0.12 | Chow 1959 |
| Emergent Herbaceous Wetland | 0.075 | 0.1 | 0.15 | Chow 1959 |

Figure 33: Manning's roughness by National Land Cover Database classification (Moore, 2011).

After retrieving NLCD data for Onion Creek (Homer, 2011), these new Manning's roughness values were re-mapped to the NLCD grid before being averaged for each Onion Creek NHDPlusV2 catchment. Using these new catchment-averaged roughness values, HAND discharges were re-computed using Manning's equation, resulting in different rating curve outputs. These outputs, with and without the depth-shift previously described, are summarized in Figure 34 for COMID 5781369. As shown, all three edited options are preferable to the currently available HAND rating curve (no depth-shift and a roughness assumption of 0.05).

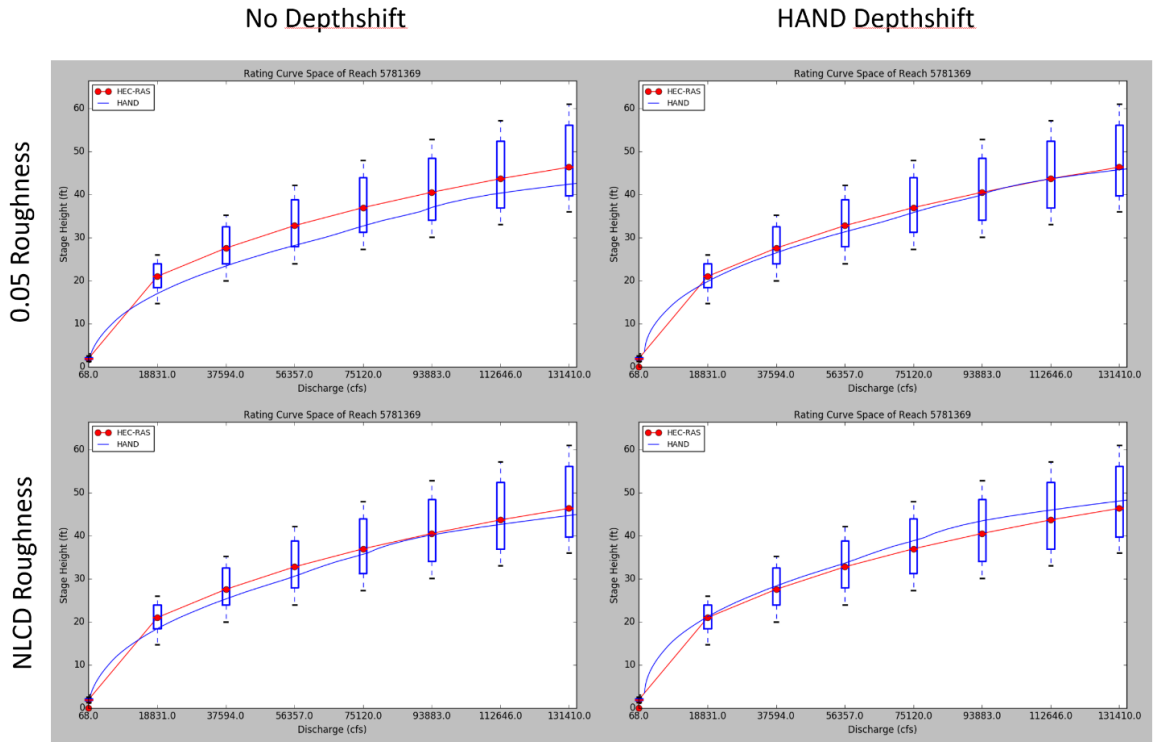


Figure 34: HAND rating curve alternatives for COMID 5781369: no depth shift and 0.05 roughness (upper left), depth shift and 0.05 roughness (upper right), no depth shift and NLCD catchment averaged roughness (lower left), and depth shift and NLCD catchment averaged roughness (lower right).

This analysis was then extended to all Onion Creek catchments, with consistently poor performers (despite the depth shift and NLCD-based catchment averaged roughness) highlighted in yellow in Figure 35. Additional details, such as the NHDPlusV2 length, NHDPlusV2 slope, topological range of DEM elevations, and number of HEC-RAS rating curves are also summarized, denoting some interesting consistencies amongst poor performers.

| COMID | Length_km | TotDASqKM | Slope | q10001c | DEM_Range_ft | HEC-RAS_Curves | Stage-Disch Ratio | NLCD_Roughness | HECRAS_Roughness |
|---|---|---|---|---|---|---|---|---|---|
| 5781385 | 14.72 | 893.6442 | 0.00159578 | 71.804 | 60.456 | 60 | 0.009448568 | 0.051516412 | 0.063 |
| 5781371 | 0.307 | 849.852 | 0.00001 | 68.932 | 12.309 | 2 | 0.102788739 | 0.054725275 | 0.06 |
| 5781369 | 4.731 | 839.9952 | 0.00136757 | 68.288 | 62.163 | 63 | 0.009887242 | 0.059360656 | 0.059285714 |
| 5781375 | 2.569 | 756.1323 | 0.00330089 | 62.82 | 54.827 | 12 | 0.009842021 | 0.078111601 | 0.062916667 |
| 5781733 | 4.072 | 742.1391 | 0.00174852 | 61.88 | 55.506 | 13 | 0.010616459 | 0.053803691 | 0.060769231 |
| 5781395 | 1.534 | 732.8745 | 0.00006518 | 61.259 | 45.451 | 7 | 0.072555345 | 0.068561551 | 0.063571429 |
| 5781403 | 2.833 | 718.9623 | 0.0017402 | 60.337 | 60.654 | 18 | 0.013221959 | 0.064629643 | 0.058611111 |
| 5781411 | 1.55 | 634.5063 | 0.00009677 | 54.593 | 47.865 | 2 | 0.032431384 | 0.068354126 | 0.0575 |
| 5781421 | 4.503 | 612.7065 | 0.00181212 | 53.075 | 66.18 | 35 | 0.00596427 | 0.050377194 | 0.058 |
| 5781939 | 0.0967 | 605.4768 | 0.00001 | 52.57 | 48.362 | 6 | 0.054850656 | 0.057701287 | 0.055 |
| 5781423 | 1.258 | 602.5392 | 0.0044833 | 52.364 | 57.539 | 3 | 0.004564837 | 0.063919108 | 0.05 |
| 5781431 | 1.224 | 468.2691 | 0.0046732 | 42.616 | 49.894 | 9 | 0.002757546 | 0.054277658 | 0.050555556 |
| 5781477 | 11.255 | 450.9342 | 0.00211816 | 41.302 | 86.828 | 22 | 0.006907033 | 0.054399551 | 0.062272727 |

Figure 35: Summary of all Onion Creek COMIDs, with consistently poor performers highlighted in yellow.

From Figure 35, the poor performers appear to generally occur for shorter reaches with smaller slopes. Notably, reaches with a smaller number of HEC-RAS cross sections are less authoritative, due to the fact that HEC-RAS cross section rating curves are highly dependent on their precise location along a reach. This means that reaches with fewer HEC-RAS cross sections have a less precise median HEC-RAS rating curve with which the respective HAND rating curve was compared. This naturally introduces error. NLCD roughness values were then similarly compared for all stream reaches with no obvious conclusions (see Figure 36).

| COMID | NLCD_11 | NLCD_21 | NLCD_22 | NLCD_23 | NLCD_24 | NLCD_31 | NLCD_41 | NLCD_42 | NLCD_43 | NLCD_52 | NLCD_71 | NLCD_81 | NLCD_82 | NLCD_90 | NLCD_95 |
|---|---|---|---|---|---|---|---|---|---|---|---|---|---|---|---|
| 5781385 | 0.46 | 21.96 | 6.09 | 6.48 | 5.46 | 0.90 | 4.55 | 1.76 | 1.36 | 14.71 | 4.22 | 16.65 | 7.68 | 7.71 | 0.00 |
| 5781371 | 0.00 | 43.96 | 9.89 | 4.40 | 0.00 | 0.00 | 5.49 | 0.00 | 0.00 | 1.10 | 2.20 | 0.00 | 0.00 | 32.97 | 0.00 |
| 5781369 | 0.74 | 6.01 | 4.60 | 3.95 | 0.99 | 11.18 | 8.47 | 8.34 | 0.00 | 26.54 | 16.16 | 1.35 | 2.69 | 8.97 | 0.00 |
| 5781375 | 2.02 | 18.25 | 1.84 | 0.99 | 0.00 | 0.00 | 12.44 | 29.04 | 0.00 | 14.54 | 2.42 | 0.00 | 4.26 | 14.21 | 0.00 |
| 5781733 | 0.16 | 24.30 | 16.58 | 11.31 | 1.45 | 0.00 | 5.04 | 2.93 | 0.00 | 20.95 | 6.24 | 0.33 | 0.58 | 10.11 | 0.00 |
| 5781395 | 0.00 | 16.69 | 13.55 | 6.07 | 0.67 | 0.00 | 15.57 | 4.44 | 0.00 | 17.71 | 2.64 | 3.20 | 0.00 | 19.45 | 0.00 |
| 5781403 | 0.00 | 16.99 | 10.55 | 17.80 | 8.87 | 0.00 | 4.20 | 11.49 | 0.00 | 14.95 | 5.93 | 3.25 | 0.67 | 5.32 | 0.00 |
| 5781411 | 0.65 | 11.96 | 10.79 | 10.66 | 0.97 | 0.00 | 5.52 | 17.35 | 0.00 | 14.88 | 14.04 | 0.00 | 0.06 | 13.13 | 0.00 |
| 5781421 | 0.07 | 20.04 | 10.11 | 8.51 | 1.23 | 0.00 | 5.07 | 4.37 | 0.00 | 24.20 | 18.11 | 3.16 | 0.25 | 4.87 | 0.00 |
| 5781939 | 1.47 | 19.88 | 6.83 | 5.64 | 1.87 | 0.00 | 9.65 | 11.86 | 0.00 | 12.68 | 20.77 | 2.08 | 2.02 | 5.24 | 0.00 |
| 5781423 | 0.00 | 18.44 | 5.75 | 3.79 | 0.89 | 0.00 | 14.92 | 13.41 | 0.00 | 15.69 | 19.59 | 0.54 | 0.00 | 6.99 | 0.00 |
| 5781431 | 0.27 | 34.91 | 9.08 | 0.16 | 0.00 | 0.00 | 10.42 | 9.99 | 0.00 | 19.39 | 4.94 | 2.52 | 0.00 | 8.32 | 0.00 |
| 5781477 | 0.38 | 13.38 | 6.65 | 5.58 | 3.05 | 2.32 | 7.75 | 6.61 | 0.00 | 27.42 | 18.43 | 3.36 | 2.46 | 2.58 | 0.03 |

Figure 36: Summary of land cover prevalence in all Onion Creek COMIDs. Column headings correspond to specific NLCD classifications.

### *3.8.2.2 NLCD Roughness by Depth*

Following the NLCD-based catchment averaged roughness approach, it was observed that an averaging of NLCD roughness values along an entire catchment was likely an inaccurate representation of reality. Instead, NLCD roughness should be computed at 1-ft depth intervals for each catchment, consequently deriving an average NLCD roughness only over the forecast flood extent area. This would more accurately describe the physical resistance which the flood was receiving from the land surface.

In order to accomplish this task, an ArcGIS ModelBuilder was developed to iterate over all flood depths, creating various flood-extent rasters containing NLCD roughness values. Notably, the NLCD dataset is available only at 30-meter resolution, while the HAND relies on NED and therefore has 10-meter resolution. This required resampling of the NLCD raster to appropriately fit over the NED rasters for meaningful comparisons between the NLCD and HAND datasets. Additional details of this model are shown in Figure 37.

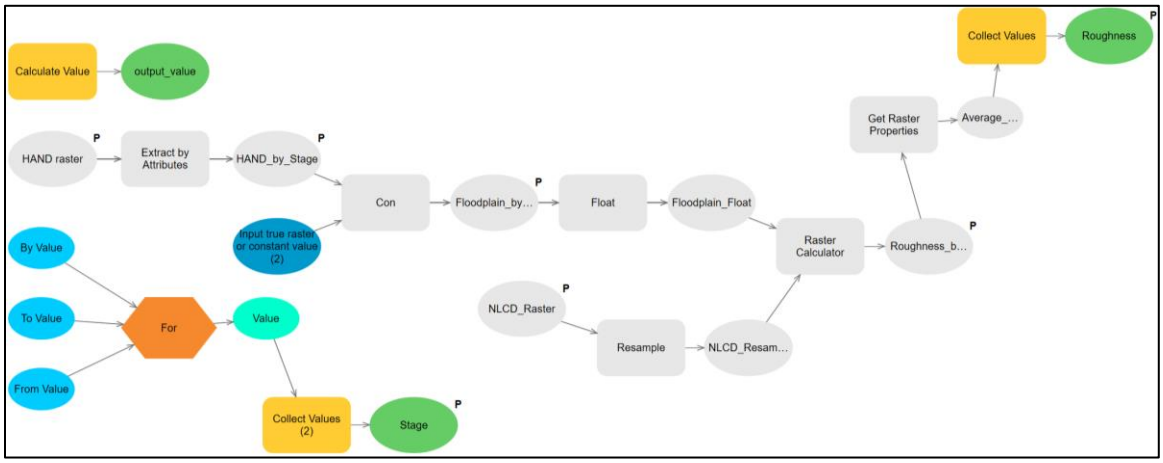


Figure 37: ArcGIS ModelBuilder workflow for automated generation of NLCD roughness by depth values.

This ModelBuilder produced different NLCD-based roughness rasters for all Onion Creak stream reaches at each different flood depth, from 0 through 82 feet (to maintain consistency with available HAND flood depth data). Three example flood inundation depths with their respective NLCD-based roughness rasters are shown in Figure 38 for COMID 5781369.

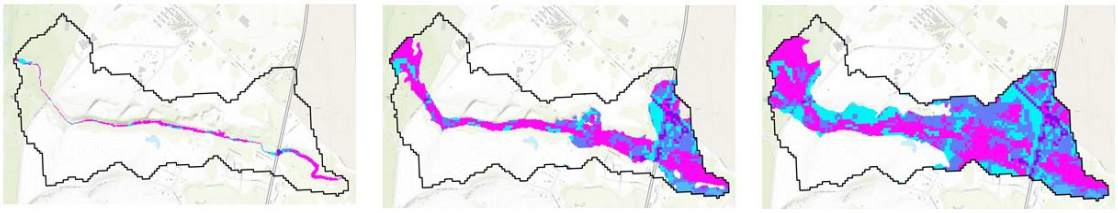

Figure 38: NLCD roughness rasters for COMID 5781369 representing HAND flood extents derived at inundation depths of 1 foot (left), 40 feet (center), and 80 feet (right).

After generating these models, a Python script was written to read through the ModelBuilder log files, retrieving the average of all NLCD roughness values within the NLCD roughness rasters. Using this methodology, averaged Manning's roughness values were computed for each COMID for all flood inundation depths between 0 and 82 feet, resulting in NLCD depth-averaged roughness values, or NLCD roughness by depth. An example rating curve generated using the previously described depth shift combined with this new NLCD roughness by depth approach for computing Manning's roughness is shown in Figure 39. While most rating curves show an improvement using this approach, this combination appears to worsen the result for this particular stream reach.

As is shown in Figure 34, the depth-shift (which has a sound theoretical basis) seems to be an improvement both when using the assumed Manning's roughness of 0.05, and when using the NLCD averaged roughness (which for this reach is approximately

0.59). The NLCD roughness by depth for this reach varies by depth from about 0.086 at 0 feet down to 0.068 at 80 feet. According to the Onion Creek HEC-RAS model, the roughness in this reach is generally 0.06, and very rarely at 0.055. Seeing as the Manning's roughness initially assumed is fairly close to the "correct" HEC-RAS roughness, as is the NLCD average roughness, this reach happens to see better agreement in these two instances. Conversely, in the case of the NLCD roughness by depth approach, the Manning's roughness values are too large initially (causing the curve to over-estimate the computed discharges), and even on the tail end of the curve this roughness remains too large.

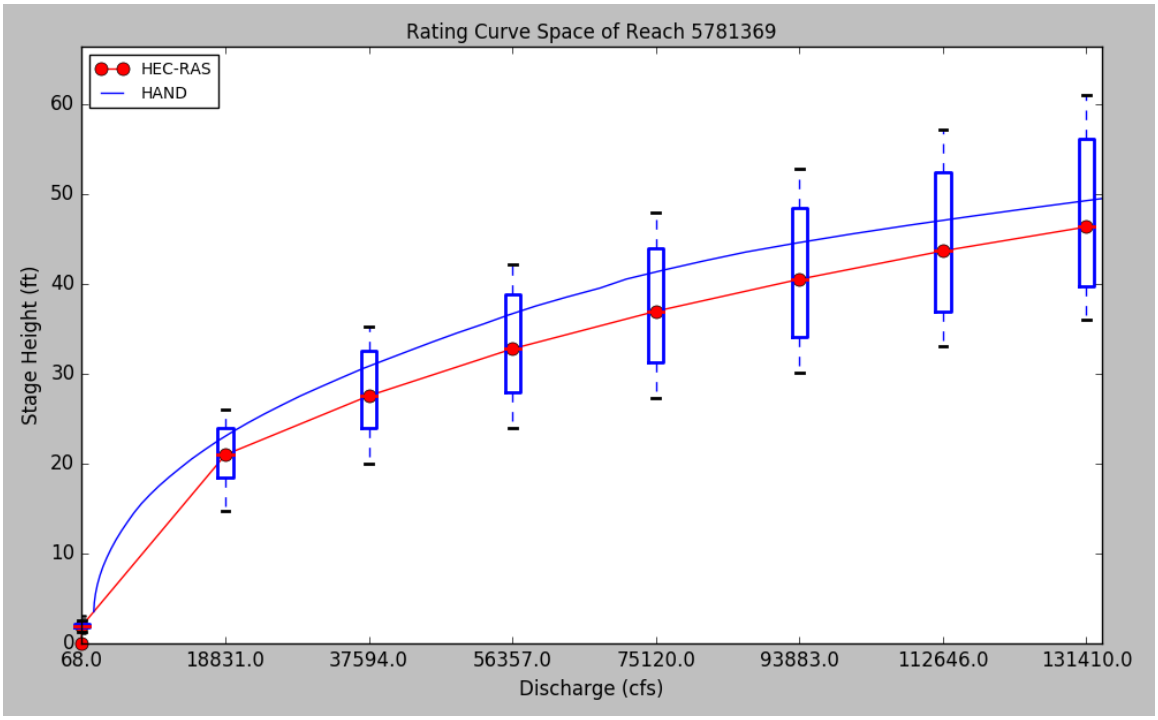


Figure 39: HAND curve using the depth shift and NLCD roughness by depth adjustments, COMID 5781369.

### 3.8.3 Slope Edits

Another problem identified in the initial rating curve analysis was the appearance of overly-gradual slopes throughout Onion Creek. As seen in Figure 35, the poor performers frequently had slopes around 0.00001, which is essentially a flat stream reach with no elevation gradient. While this is theoretically possible, the results previously found in the Onion Creek stream profile Figure 24) show that the DEM and FEL-derived stream profiles vary significantly more than the HEC-RAS stream profiles. This decreasing overall confidence in the NHDPlusV2 slopes due to their jaggedness.

#### *3.8.3.1 DEM Slope*

In attempting to correct for this, a more detailed slope analysis was conducted to generate alternative slopes to those available through the NHDPlusV2. This was done by averaging hydrologic slopes along DEM-derived channels for each catchment, where a DEM-derived flowline is simply a 1-cell wide channel defining the lowest points of drainage passing through a catchment. These DEM-derived channels are published on the HAND webpage as a ".src" file for all HUC-6 regions (NFIE, n.d.). An additional dataset collected from the HAND webpage was the ".slp" file containing slope data; this dataset describes the hydrologic slope, or the steepest vertical slope, of each cell in the area (NFIE, n.d.).

First, the data was cleaned by extracting only data within the catchments in question. The hydrologic slope values were then conditionally selected solely where they intersected with the DEM-derived flowline, ultimately returning slopes for every cell along each catchment's flowline. These slopes-along-each-flowline were averaged together for each reach, resulting in an average DEM-derived slope over each stream reach, in theory roughly equivalent to the NHDPlusV2 slopes (see Figure 40).

| COMID | DEM_Slope_Min | DEM_Slope_Max | DEM_Slope_Mean | DEM_Slope_StDev |
|---|---|---|---|---|
| 5781369 | 0 | 0.093854 | 0.001769 | 0.008561 |
| 5781371 | 0 | 0.041986 | 0.008040 | 0.012392 |
| 5781375 | 0 | 0.062612 | 0.002252 | 0.009426 |
| 5781385 | 0 | 0.150538 | 0.001394 | 0.007817 |
| 5781395 | 0 | 0.087553 | 0.003281 | 0.011267 |
| 5781403 | 0 | 0.049154 | 0.001815 | 0.005938 |
| 5781411 | 0 | 0.095084 | 0.002031 | 0.010825 |
| 5781421 | 0 | 0.101771 | 0.001609 | 0.008168 |
| 5781423 | 0 | 0.202001 | 0.002751 | 0.019010 |
| 5781431 | 0 | 0.184441 | 0.007994 | 0.019702 |
| 5781477 | 0 | 0.194736 | 0.002213 | 0.010369 |
| 5781481 | 0 | 0.045980 | 0.001017 | 0.005841 |
| 5781733 | 0 | 0.247530 | 0.002619 | 0.018191 |
| 5781931 | 0 | 0.000470 | 0.000078 | 0.000192 |
| 5781939 | 0 | 0.000000 | 0.000000 | 0.000000 |

Figure 40: DEM-derived average flowline slopes for all Onion Creek catchments.

#### *3.8.3.2 Slope Complications*

Observing the results in Figure 40, there is clearly a problem with the very last reach, COMID 5781939. The slope of this reach is zero, which – whether it makes physical sense or not – will cause problems in the HAND model at this catchment, resulting in very extremely inaccurate rating curves for flood prediction.

In attempting to understand the reason for this zero slope, a closer analysis of COMID 5781939 was conducted. Plotted in Figure 41 is COMID 5781939 with a green outline denoting the catchment, blue-and-orange lines denoting the DEM-derived flowline, and the black-and-white background denoting hydrologic slope values across the entire reach (black is zero slope, white is 100% slope). Blue cells along the flowline have a slope of zero, while orange cells represent any positive, non-zero slope. From Figure 41 the reason for a zero average slope of the reach becomes very clear: all hydrologic slope values

along the flowline for this catchment have a value of zero, thus resulting in an average hydrologic slope of zero along the whole reach. Similarly, while there are slope values on the two neighboring catchments, there are apparently a very large fraction of data points with zero slope in these reaches as well. This is problematic and currently unresolved.

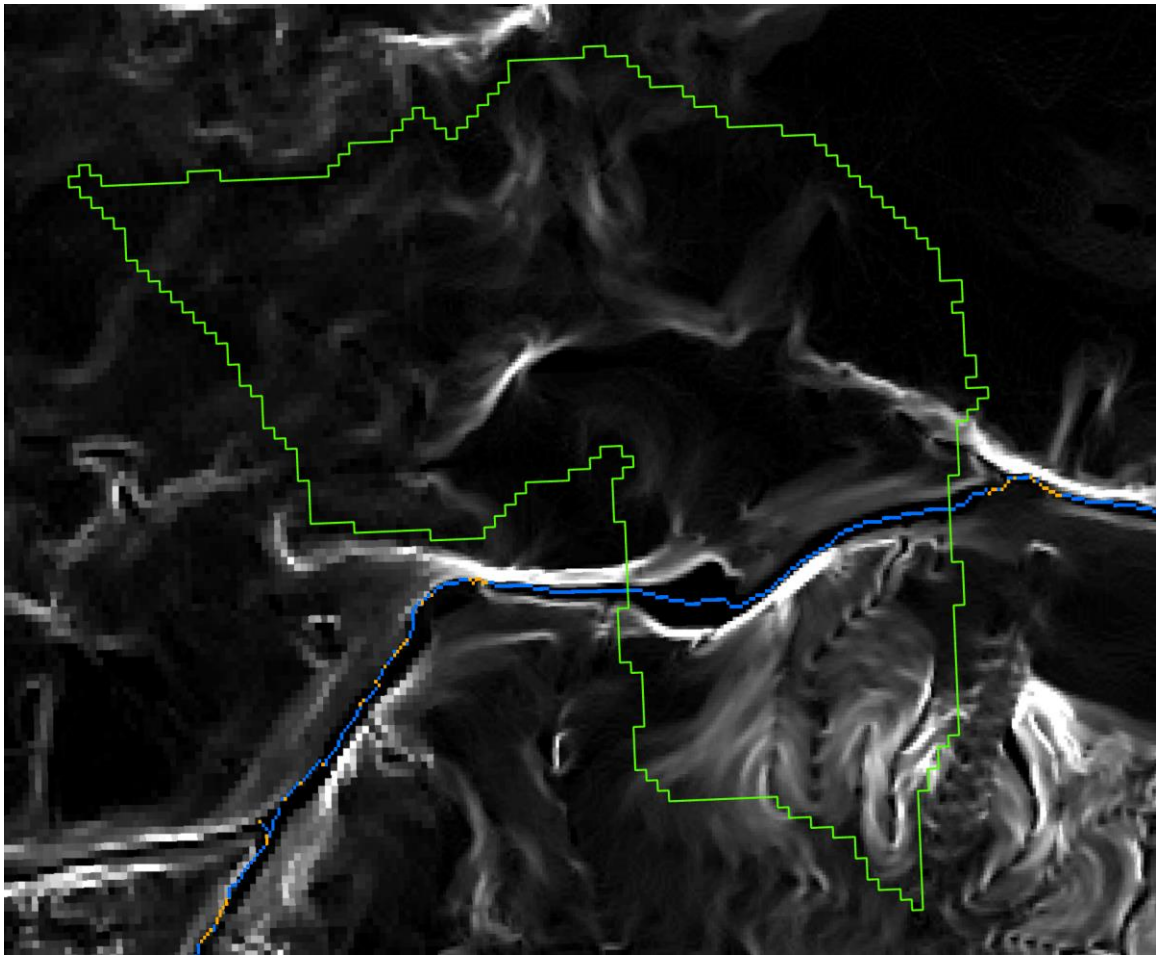

Figure 41: Hydrologic slope values in and around COMID 5781939.

#### *3.8.3.3 Catchment-Averaged and Nearest-Neighbor Slopes*

In attempting to resolve this issue of zero-slopes, nearest-neighbor slopes were computed as averages of each slope with its two (or one, in the case of the two stream

reaches on either end of Onion Creek) neighboring stream reach's slopes. This was attempted hoping that neighboring catchments would have similar slopes. Hypothetically, this would result in nearest-neighbor averages simply smoothing out the results and simultaneously taking care of any zero-slope catchments by giving them a small positive slope. The results of this analysis are shown in Figure 42, representing both NHDPlusV2 and DEM-derived slopes alongside their nearest-neighbor slopes.

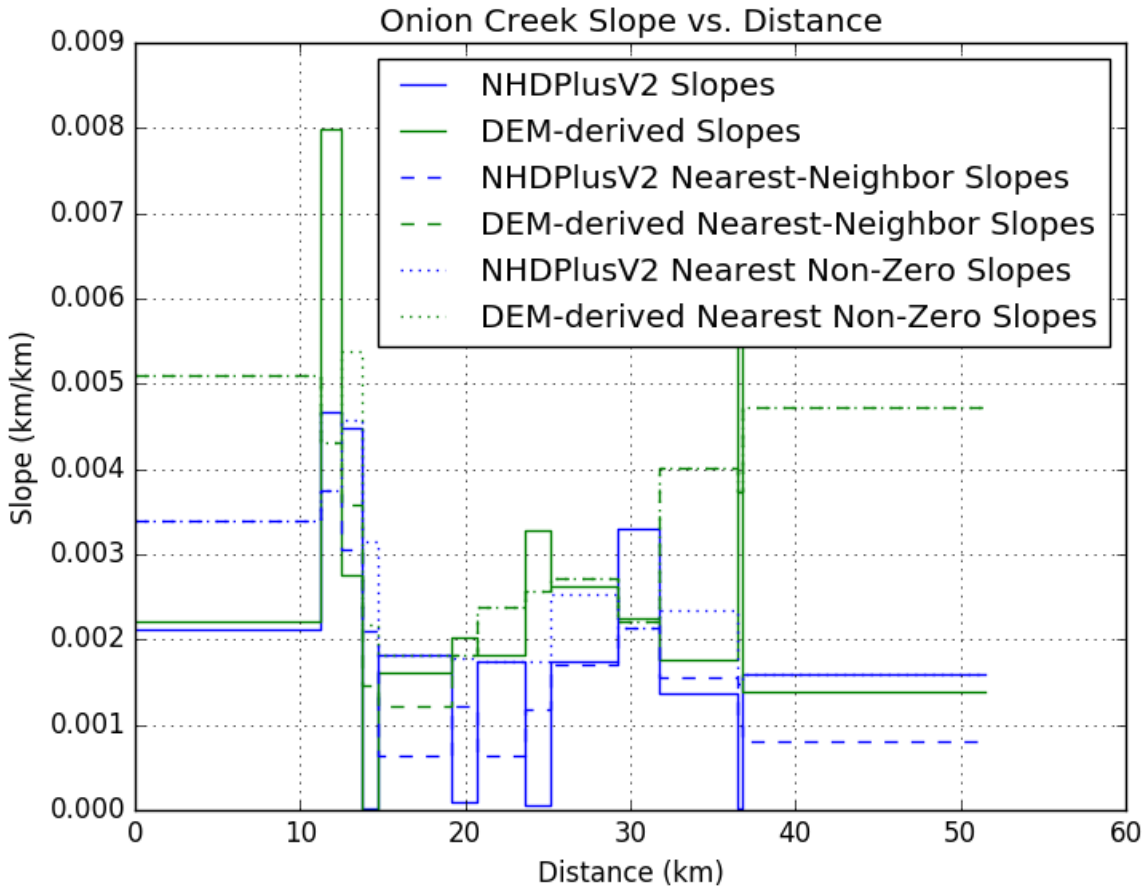


Figure 42: NHDPlusV2 and DEM-derived slopes along Onion Creek.

From Figure 42 it is clear that the slopes are incredibly variable along Onion Creek. Not only are the NHDPlusV2 and DEM-derived slopes significantly different for most

stream reaches, but the slopes from one point as compared to another point a few kilometers downstream are often unrealistically different. Plotted in Figure 42 for additional information is also a third option explored in the later phases of this project, describing the nearest non-zero neighbors. This line shows the nearest-neighbor averaged slopes with all 0 or 0.00001 (in the case of NHDPlusV2) slope values ignored. Apparently this avoidance of problematic stream reaches does not seem to have significantly large deviations from the nearest-neighbor slopes overall, and these deviations are still sporadically rising and falling throughout the reach (which is physically improbable).

Further comparison to the previously-computed stream profile Figure 24 confirm this problem, with the DEM and FEL-derived stream profiles varying significantly more than the HEC-RAS stream profile. A summary of the resulting rating curves generated for COMID 5781369 using these different slopes can be seen in Figure 43.

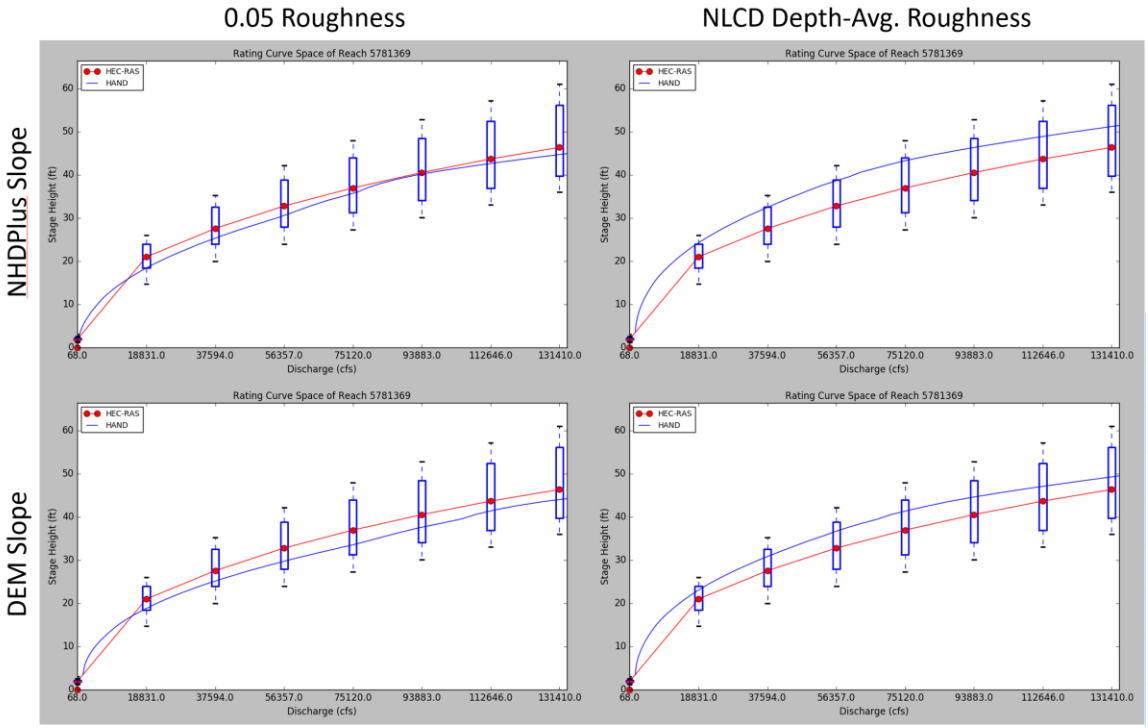


Figure 43: HAND rating curve alternatives for COMID 5781369: NHDPlusV2 catchment-averaged slope and 0.05 roughness (upper left), NHDPlusV2 catchment-averaged slope and NLCD roughness by depth (upper right), DEM-derived catchment-averaged slope and 0.05 roughness (lower left), DEM-derived catchment-averaged slope and NLCD roughness by depth (lower right).

# Chapter 4: Results

## 4.1 Preliminary Rating Curves

Preliminary rating curve results are focused on the initial study area and the data collected for that region. One particular different is the use of the earlier HEC-RAS curves with 5 linearly-interpolated points.

### 4.1.1 Rating Curves

An example summary of all preliminary rating curve data collected for the three focus COMIDs is shown in Figure 44. From observation there appears to be a consistent trend that USGS and HAND cross-sections are in the lower ranges of the HEC-RAS curve spread. Rationally, this may mean that USGS gages are placed at wider cross-sections (where, generally, stage-height increases less as discharge increases). This may make sense from a field-installation and observation standpoint: data can be collected from much larger storms (ie. higher discharges) without the storm destroying the gage. Despite this seemingly rational explanation, there is no way of knowing whether this is true in practice or not (save viewing all of the USGS gages in the field). However, if this were known, there may be potential for generalizing the USGS rating curves for the rest of the nation, by taking into account where a USGS gage would be most likely placed and using those geometries for rating curve comparisons. This would not necessarily improve the accuracy of rating curves, but it would at least maintain consistency with USGS practices.

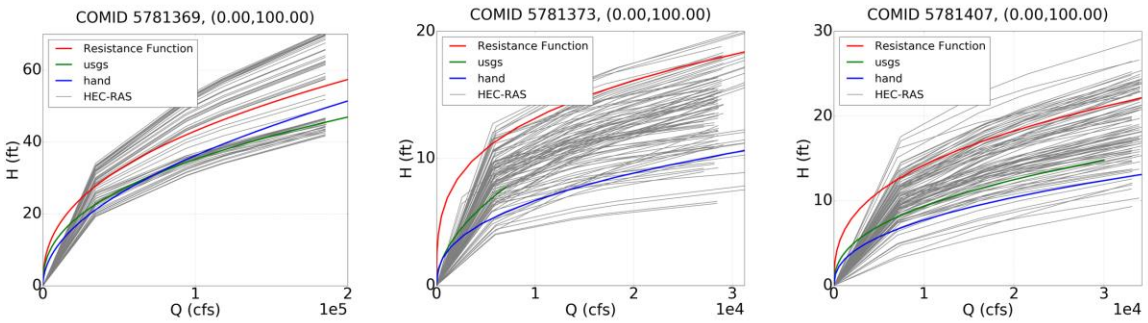


Figure 44: Preliminary HAND, USGS, and HEC-RAS curves, as well as the initially constructed HEC-RAS "resistance function" for COMIDs 5781369, 5781373, and 5781407.

### 4.1.2 Boxplots

Preliminary box plots were also created for all stream reaches in the Onion Creek watershed, with three examples shown in Figure 45. From these box plots it is clear that not only is there a large spread of HEC-RAS data, but some COMIDs have incredibly large outliers. These outliers, which tend to appear more at higher stage heights, are likely related to the power-law regression used to fit the rating curves: as stage height increases, discharge values of the power-law fit quickly approach infinity, thus producing some of the results seen in COMIDs 5781373 and 5781407.

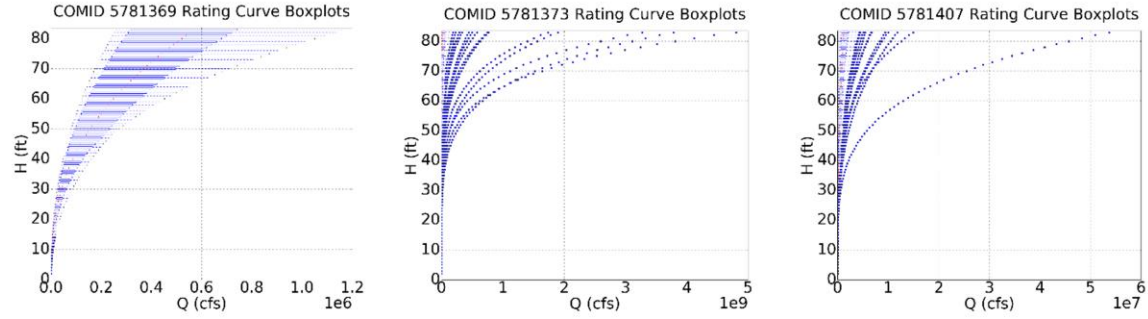


Figure 45: Preliminary HEC-RAS rating curve spread represented as boxplots for COMIDs 5781369, 5781373, and 5781407.

### 4.1.3 Scaling Analysis

Specifically observing COMID 5781369, Figure 46 shows the river channel split into 5,000-foot lengths. The USGS, HAND, and Resistance Function curves shown are all at the entire stream-reach scale, whereas the HEC-RAS curves shown are only relevant to the scale in the image title; these titles are measured in percent-length, meaning 32 corresponds to a length 32% along the stream reach. As such, the first image shows only the HEC-RAS rating curves from 0 through 32.21% of the stream reach, or roughly the first third.

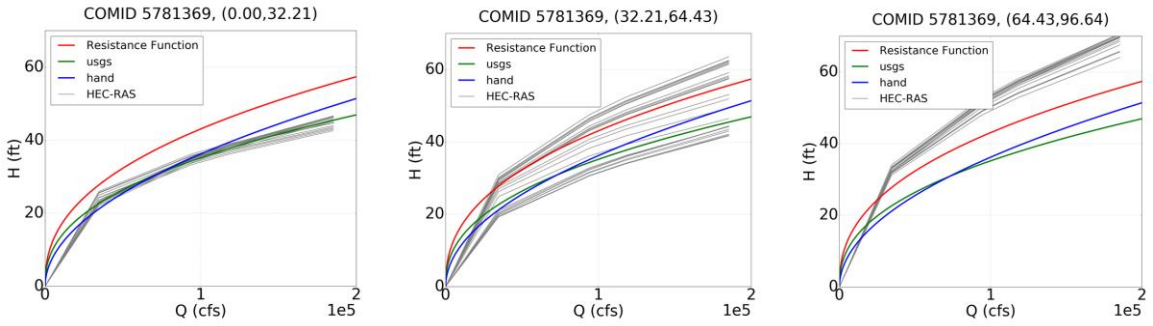


Figure 46: Preliminary HAND, USGS, and "resistance function" rating curves as compared to HEC-RAS rating curves along specific portions of COMID 5781369.

Notably, similar images have been created for all other stream reaches in the Onion Creek watershed containing both HEC-RAS cross-sections and USGS gage data. COMID 5781369 shown in Figure 44 is one of the best performers of the group in terms of consistent HEC-RAS cross sections along the stream length (meaning that the cross sections seem to look similar to their cross section neighbors within the 5,000-foot scale used). Consequently, for this stream reach, the result ends up showing that the USGS rating curve (which is in the first third of this catchment) matches up fairly nicely with the nearby HEC-RAS cross-sections. However, this apparent matching is not consistent for the other

stream reaches analyzed; the majority of the other COMIDs experienced much more variability, with no clear consistency arising from the data.

### 4.1.4 Manning's Roughness Optimization

In an optimization effort to fit HAND rating curves to USGS curves, Manning's roughness coefficient was treated as a parameter which could be tweaked to minimize the least-squares difference between these rating curves. This was a preliminary analysis to determine if a simple manipulation of Manning's roughness would suffice for accurately approximating the USGS rating curves, and subsequent work was intended to expand these results to the CONUS. Figure 47 shows these preliminary results.

| COMID | roughness |
|---|---|
| 5780099 | 0.4 |
| 5781353 | 0.2 |
| 5781369 | 0.15 |
| 5781373 | 0.35 |
| 5781401 | 0.15 |
| 5781407 | 0.07 |
| 5781431 | 0.45 |
| 5781731 | 0.35 |

Figure 47: Summary of optimized Manning's roughness values for stream reaches in the Onion Creek watershed.

For the most part, these values are very far from normal (Chow, Maidment, & Mays, 1988), with an average of optimal Manning's roughness of 0.265 for the COMIDs assessed. Due to the enormity of these results, it seems that a simple minimization of least-squares is not an acceptable approach. Additionally, even if this approach had been accepted as a physically reasonable Manning's roughness adjustment, the generalization

of this solution to a national scale would have been remarkably difficult; there are simply not enough USGS gages to create a meaningful machine learning training dataset from (let along validation and testing datasets).

### 4.2 Cross Sections

Interesting comparisons between HAND and USGS cross sections were also conducted, such as that shown in Figure 48. This comparison looks fairly good, reinforcing the belief that the HAND methodology is consistently missing some area at the bottom of each cross-section (see right side of Figure 48, with GZF depth correction implemented). As is also clear from this comparison, the GZF shift is necessary for any sort of meaningful comparison between HAND and USGS cross-sections, because without this shift the cross-sections do not relate in any visibly meaningful way (as in the case of the left image in Figure 48).

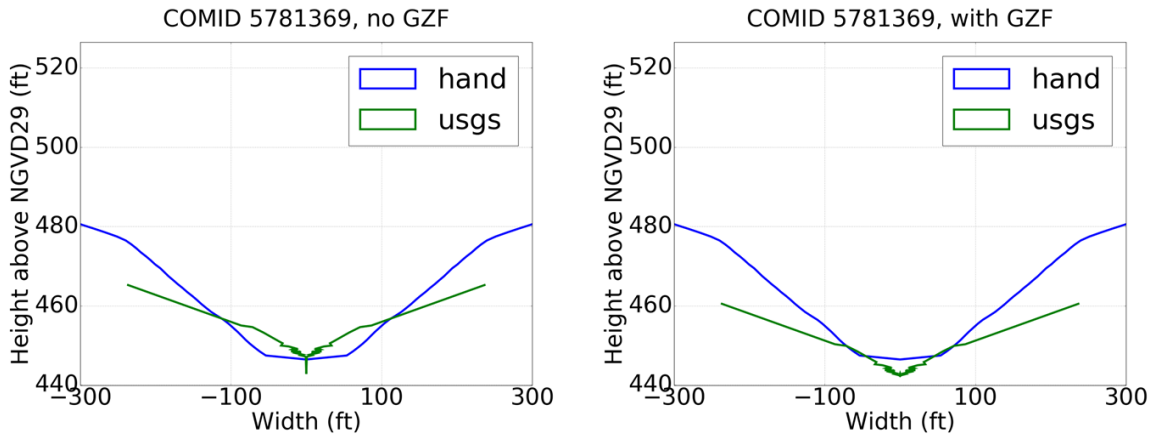


Figure 48: HAND (blue) and USGS (green) cross sections with (left) and without (right) a GZF depth shift correction for COMID 5781369.

Due to this restriction, and due to the lack of available GZF shift data for the stream reaches here in question, there are few cross section results, most of which look worse than

that shown in Figure 48. Many results have cross sections that are tens of feet separated due to unavailable depth shifts or other complications. As such, no HAND rating curve recommendations can be recommended based on these cross sections.

## 4.3 Final Rating Curves

Analyzed over the revised study area and using the more complex HEC-RAS reach-averaged rating curves for comparison, this final analysis summarizes a meaningful way to compare the various options presented.

### 4.3.1 Rating Curves

A visual assessment of fit was first used to determine which combination of roughness and slope correction methodologies would result in the best HAND rating curves (as compared to the median HEC-RAS rating curves) for Onion Creek as a whole. An example visualization is shown in Figure 49, comparing different roughness alternatives with NHDPlusV2 or DEM-derived catchment-averaged slopes. The nearest-neighbor slopes are not shown on this particular plot to avoid clutter, but they can be analyzed in a similar way as well.

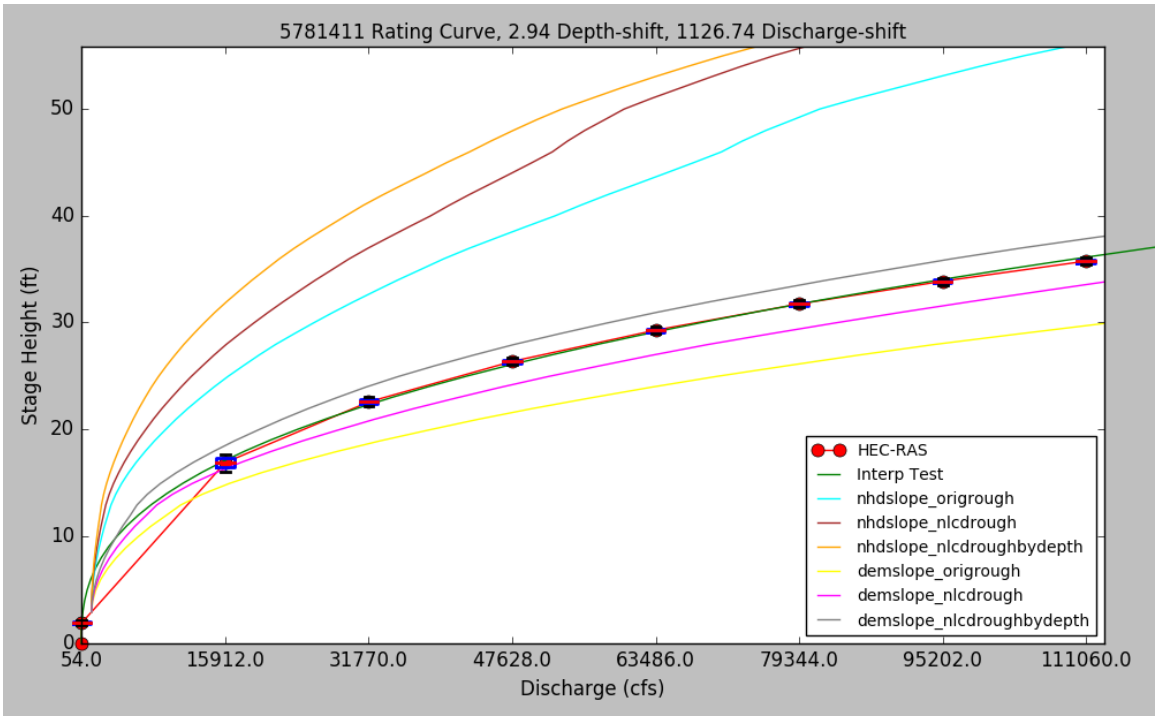


Figure 49: Example of various HAND-derived rating curves as compared to the HEC-RAS rating curve and its power-law fit curve for COMID 5781369.

While it is clear that the best curves for this reach are either the DEM-derived slope with the NLCD-based roughness-by-depth approach, or the DEM-derived slope with a reach-averaged NLCD-based roughness, this is not consistent when compared amongst all stream reaches. As such, a least-squares approach was used to assess performance, assessing which approach minimized the least-squares difference for a majority of the stream reaches along Onion Creek.

### 4.3.2 Least-Squares Difference Analysis

In order to conduct a least-squares difference minimization, first a multitude of data points must be gathered along the curves to be compared. The HAND rating curves have 83 data points, one for each whole number stage height between 0 and 82 feet, whereas the HEC-RAS rating curves have only eight evenly-spaced data points at decimal stage heights

along the curve. Therefore, in enabling a comparison between these two curves, a power-law curve was first fit to each HEC-RAS rating curve to enable queries upon it at all 1-foot stage height intervals.

Using power-law curves fitted to each catchment's averaged HEC-RAS rating curve, a more mathematically meaningful comparison of least-squares differences could be made between the median HEC-RAS rating curve and various HAND-derived rating curves. Notably, these power-law fits did not always perfectly describe the rating curves they were derived from. An example of a very good fit and one of the worst fits within Onion Creek are shown in Figure 50; most rating curves fell somewhere on the spectrum between these two examples in terms of goodness of fit. This introduces some error into the least-squares difference methodology here applied, yet this power-law fit was still considered to be superior as compared to the linear interpolation seen in red in Figure 50, particularly seeing as the power-law fit fairly accurately describes the lower stage heights of the rating curve, while the linear interpolation shortcuts this portion of the curve.

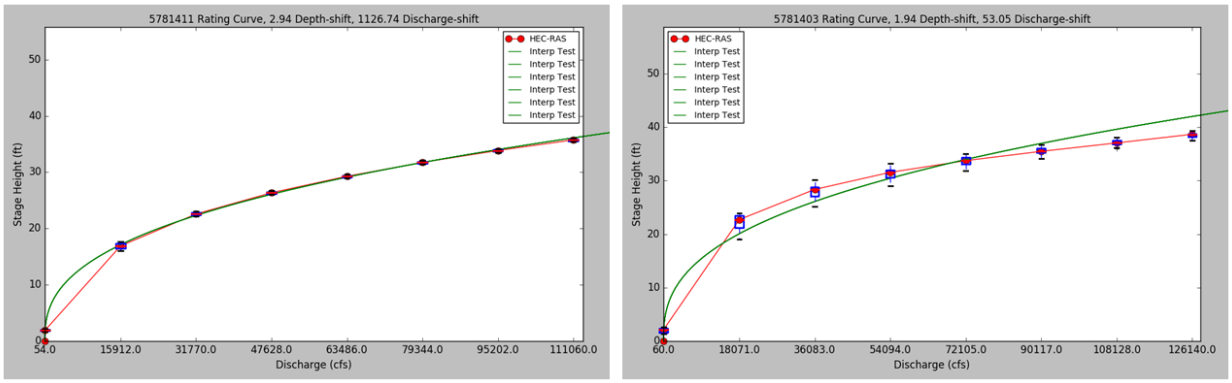


Figure 50: Two example HEC-RAS rating curves showing a power-law curve fitted to the eight linearly-interpolated HEC-RAS data points. COMID 5781411 (left) shows an exceptionally good fit, while COMID 5781403 (right) shows a relatively poor fit.

Once the HEC-RAS rating curves were fit to a power-law function, squared discharge differences were summed for all 1-foot stage height intervals up to the final HEC-RAS data point; this distinction is important, as it removed the errors that would be experienced as the power-law curves approached infinite discharges for marginally larger stage heights. This least-squares difference approach was then applied for all potential HAND rating curves as compared to a stream reach's power-law fit HEC-RAS rating curve. These least-squares differences were then ranked for each COMID, resulting in an ordering as shown in Figure 51.

| COMID | Best | ... | ... | ... | ... | Worst |
|---|---|---|---|---|---|---|
| 5781477 | demslope_nlcdroughbydepth | nhdslope_nlcdroughbydepth | nhdslope_nlcdrough | demslope_nlcdrough | nhdslope_origrough | demslope_origrough |
| 5781431 | nhdslope_nlcdroughbydepth | demslope_nlcdroughbydepth | nhdslope_nlcdrough | nhdslope_origrough | demslope_nlcdrough | demslope_origrough |
| 5781423 | demslope_nlcdroughbydepth | nhdslope_nlcdroughbydepth | demslope_nlcdrough | nhdslope_nlcdrough | demslope_origrough | nhdslope_origrough |
| 5781939 | nhdslope_origrough | nhdslope_nlcdrough | nhdslope_nlcdroughbydepth | demslope_origrough | demslope_nlcdrough | demslope_nlcdroughbydepth |
| 5781421 | demslope_nlcdroughbydepth | demslope_nlcdrough | demslope_origrough | nhdslope_nlcdroughbydepth | nhdslope_nlcdrough | nhdslope_origrough |
| 5781411 | demslope_nlcdroughbydepth | demslope_nlcdrough | nhdslope_origrough | nhdslope_nlcdrough | nhdslope_nlcdroughbydepth | demslope_origrough |
| 5781403 | nhdslope_nlcdroughbydepth | demslope_nlcdroughbydepth | nhdslope_nlcdrough | demslope_nlcdrough | nhdslope_origrough | demslope_origrough |
| 5781395 | demslope_nlcdroughbydepth | nhdslope_origrough | nhdslope_nlcdrough | nhdslope_nlcdroughbydepth | demslope_nlcdrough | demslope_origrough |
| 5781733 | nhdslope_nlcdroughbydepth | nhdslope_nlcdrough | nhdslope_origrough | demslope_nlcdroughbydepth | demslope_nlcdrough | demslope_origrough |
| 5781375 | nhdslope_nlcdroughbydepth | nhdslope_nlcdrough | demslope_origrough | demslope_nlcdrough | demslope_nlcdroughbydepth | nhdslope_origrough |
| 5781369 | demslope_nlcdroughbydepth | nhdslope_nlcdrough | nhdslope_nlcdroughbydepth | demslope_nlcdrough | nhdslope_origrough | demslope_origrough |
| 5781371 | nhdslope_origrough | nhdslope_nlcdrough | nhdslope_nlcdroughbydepth | demslope_nlcdroughbydepth | demslope_nlcdrough | demslope_origrough |
| 5781385 | demslope_nlcdroughbydepth | nhdslope_nlcdroughbydepth | demslope_nlcdrough | demslope_origrough | nhdslope_nlcdrough | nhdslope_origrough |

Figure 51: Organization of least-squares difference from best to worst HAND rating curve candidate for each COMID along Onion Creek.

From Figure 51, it is fairly clear that, when paired with the depth shift and some form of slope adjustment, the NLCD roughness by depth ("nlcdroughbydepth") methodology is an improvement over the 0.05 Manning's roughness assumption previously used. While these changes to the Manning's roughness seem to consistently improve results, understanding which slope is the best performer is more difficult. In the "Best" column, seven of thirteen results show the DEM-derived slope as being the winner. However, seeing as this represents only 54% of a very small sample, the second-best column was also assessed, showing that the NHDPlusV2 slope seems superior overall. This discrepancy creates some confusion and fails to inform any valid conclusions.

In a more useful visualization, box plots were generated to explore the spread of least-squares values when assessing all catchments along Onion Creek (see Figure 52, where the y-axis represents the least-squares differences in trillion cubic feet per second; smaller values correspond to minimal least-squares differences). Plotting only catchment-averaged slopes, the NHDPlusV2 catchment-averaged slope and the NLCD roughness by depth approaches together seemed to minimize the deviations of the rating curve least-squares differences significantly more than the other methods. Notably, as mentioned, each least-squares regression was computed only up to the furthest HEC-RAS point for each stream-reach to avoid extreme power-curve deviation at larger stage-heights. This resulted in least-squares values likely deviating in magnitude from reach to reach, which may have caused some of the extreme outliers shown in Figure 52. However, because this value was consistent for all methodologies for any given reach (because this cut-off is based on the HEC-RAS rating curve, not the HAND rating curve), this difference was deemed to be acceptable.

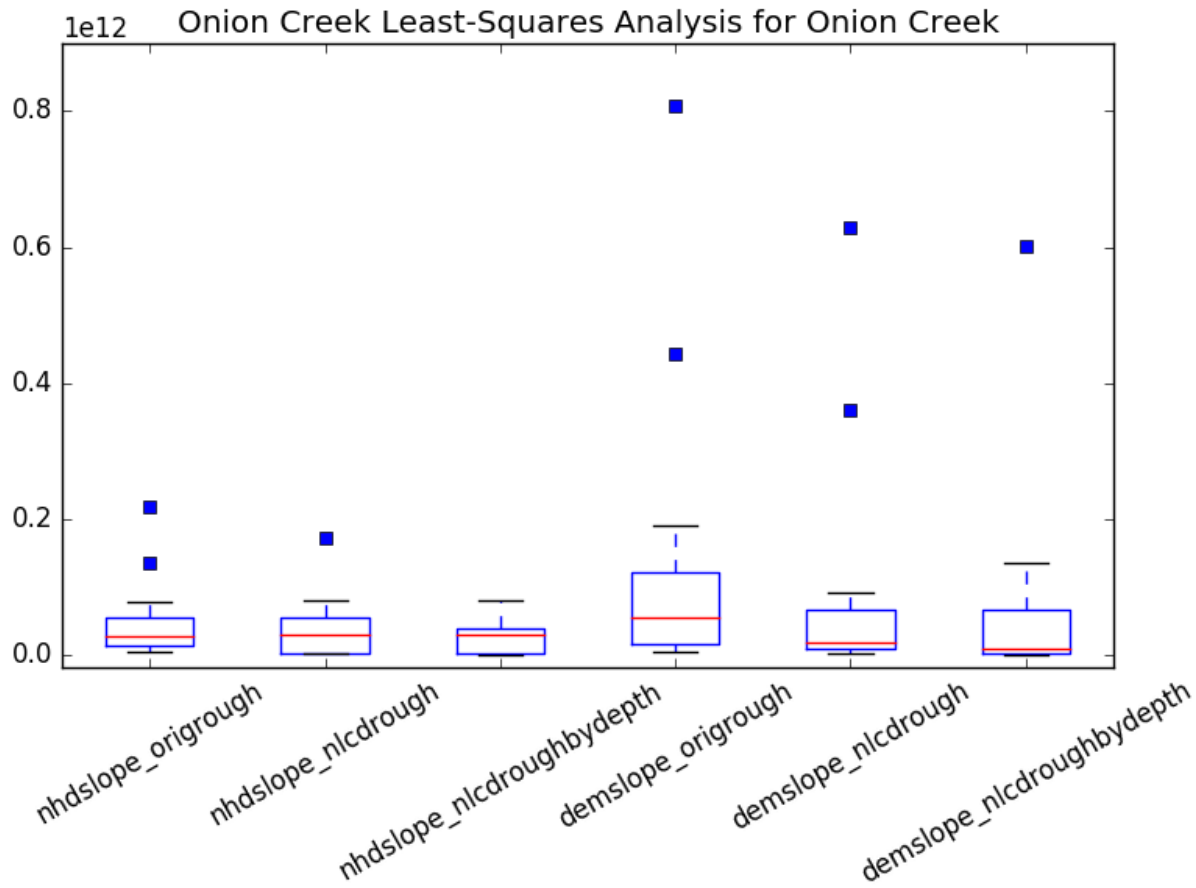


Figure 52: Box plots representing the spread of least-squares differences for all COMIDs organized by rating curve adjustment type.

While conclusive results as to the best of the six methods may or may not be valid, it is fairly clear that the NLCD roughness adjustments tend to outperform the original 0.05 roughness assumption for both slope alternatives. The comparison is still unclear as to slope performance, but the NHDPlusV2 slopes seem to perform best.

In remembering that COMID 5781939 was a problematic reach with a miniscule (NHDPlusV2) or zero (DEM-derived) slope, this particular reach was treated as an outlier and was temporarily removed from the analysis. After ignoring COMID 5781939, the resulting performance of the Onion Creek catchments significantly improved (see Figure

53), showing that, if this problematic reach is ignored, the NLCD roughness by depth approach seems to be the clear winner over the other approaches. While the DEM-derived slope seems to perform marginally better than the NHDPlusV2 slopes overall, the conclusion as to which is the better approach remains unclear.

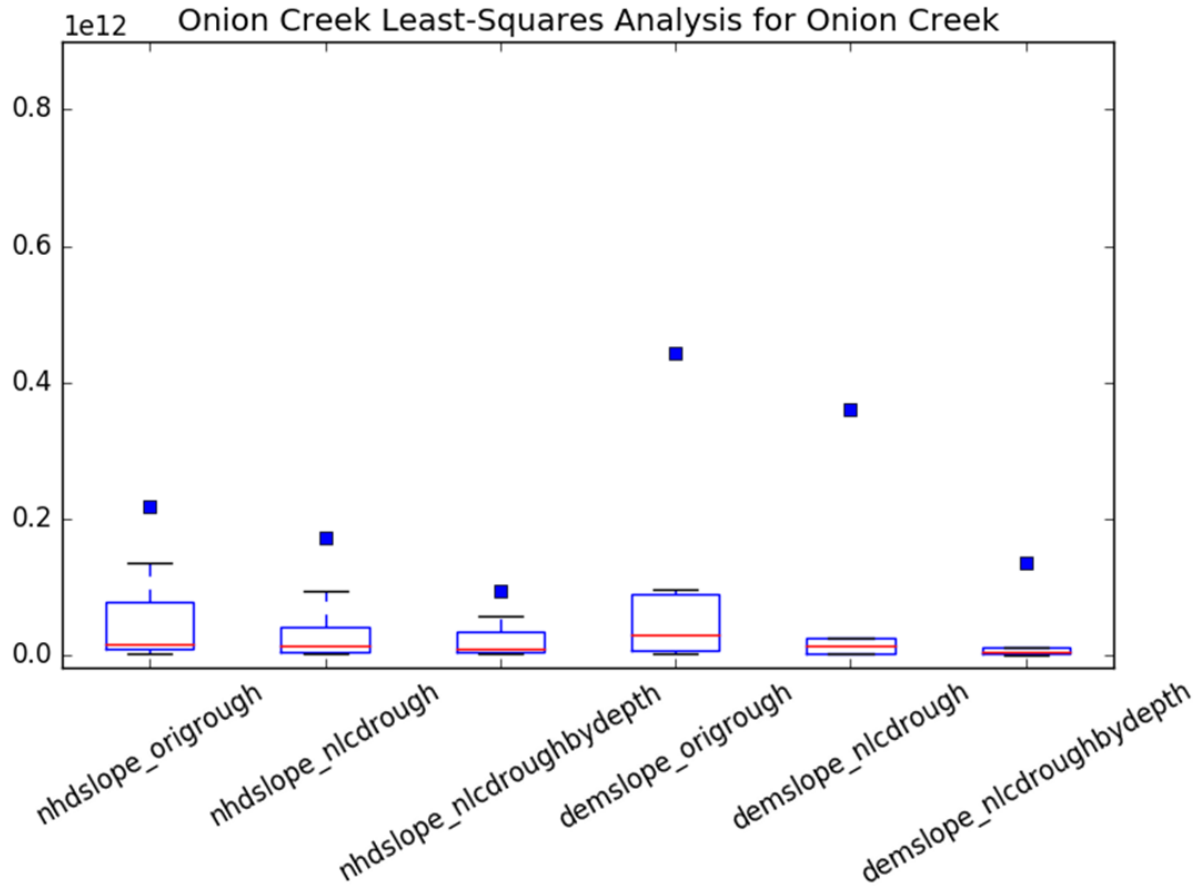


Figure 53: Box plots representing the spread of least-squares differences for all COMIDs excluding COMID 5781939.

In attempting to resolve these slope complications, the previously-calculated catchment-averaged and nearest-neighbor slopes were used in conjunction with the NLCD-based roughness by depth approach to generate a new set of box plots strictly comparing

the influence of different slopes (see Figure 54). COMID 5781939 was added back in again for this analysis, as the real purpose of this project is to determine a generalizable approach for resolving all rating curve corrections. As such, even the problematic reaches need to be included.

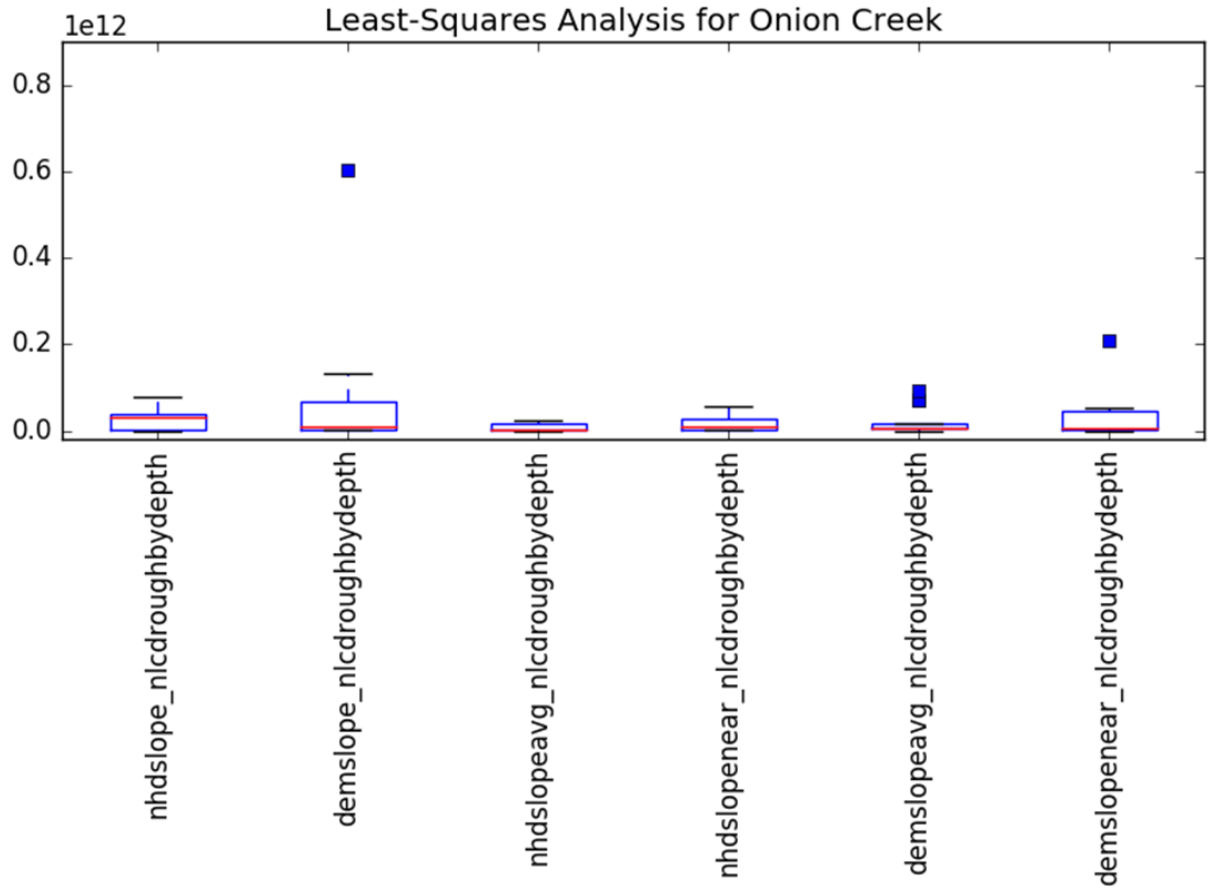


Figure 54: Box plots representing the spread of least-squares differences for all COMIDs, specifically comparing various slope alternatives. The NLCD roughness by depth approach is used for all of these box plot alternatives.

From this comparison, the NHDPlusV2 reach-averaged slope is clearly the best performer. However, despite this improved performance, the nearest-neighbor approach

would likely be the simplest to generalize and implement on a large scale. Consequently, the NHDPlusV2 nearest-neighbor slope is considered to be the best all-around performer, though further research is highly recommended before adapting these changes.

# Chapter 5: Conclusions

A major finding of this research is that, while USGS rating curves are largely beneficial for spot-checking of models at specific locations, they are largely ineffective for national-scale flood mapping due to their relative spatial scarcity. Consequently, while precisely-derived rating curves from highly detailed cross section field measurements may be beneficial to small-scale studies, they should not be relied upon for large-scale hydrological implementations. In the end, a generalizable flood extent modeling approach that is mostly correct and operational is vastly preferable to a system that is perpetually being improved and never being delivered.

An additional finding from HEC-RAS rating curve exploration is also interesting. HEC-RAS rating curves along each NHDPlusV2 stream reach have much more resolution than the more sparse USGS rating curves. Consequently, if a method existed to ingest all HEC-RAS models throughout the nation for detailed river channel modeling, then the NHDPlusV2 stream reaches might all feasibly be highly understood in the near future. Similarly, if the theoretical reasons for at-a-station hydraulic geometry relations are ever agreed upon, cross section geometries may be computed at a very high spatial scale. However, while this may sound very interesting from a hydrological perspective, it has here been discovered that an incredibly high level of detail may in fact be disadvantageous. The large quantity of HEC-RAS rating curves had such an enormous spread for each NHDPlusV2 stream reach (and this spread was consistently large, even for smaller subsets of these stream reaches) that averaging these rating curves over the entire stream reach was the only feasible method for utilizing them. Ironically, an excess of data is also seemingly unbeneficial.

A third and very important finding is that both the NHDPlusV2 and DEM-based slopes utilized in this analysis were found to be unreasonable for Onion Creek. The tremendous amount of variation occurring along this one reach, as well as the fairly common zero-slope reaches (or 0.00001 m/m for NHDPlusV2), is hydrologically and bathymetrically unlikely. From the Onion Creek stream profile generated in this research, it is apparent that the HEC-RAS model has a significantly more consistent (and realistic) understanding of bed elevation which is not captured by the National Elevation Dataset. An alternative methodology is likely needed to resolve this issue, with nearest-neighbor averages presenting a possible step in the correct direction.

Regarding the extensive analysis of different proposed solutions for improving HAND rating curves, it is clear that some newly-proposed approaches may be advantageous. In particular, the NLCD roughness by depth approach seems to improve Onion Creek rating curves significantly on average. Similarly, while the results were not nearly as conclusive, the NHDPlusV2 slopes seem preferable to the DEM-derived slopes, and the problem of tremendously small slope values can possibly be decreased through nearest-neighbor slope averaging.

While these results seem to have clear benefits to national-scale HAND rating curve improvements, their exploration at the Onion Creek scale are insufficient for large scale implementation. To further this research, these findings must be explored for other stream reaches, preferably in other regions with different climates, topologies, and geographies than those present in Onion Creek. Finally, if certain approaches seem to consistently improve HAND rating curves across regions, a full analysis must take place at the national scale, including all 2.67 million NHDPlusV2 stream reaches, before implementation of these new methodologies should be applied.

Though the purpose of this research was to improve the process of generating HAND rating curves on a national scale, many incompatible approaches ended up becoming the most informative findings. From limited USGS data availability and extensive HEC-RAS data availability, the NHDPlusV2 stream reach-averaged rating curve approach was very much validated; this level of resolution is ideal for the implementation of flood extent mapping using current technologies. Additionally, potential solutions relying on other national datasets have been explored, particularly the NLCD roughness approaches and the DEM-derived slopes, which both seem to present feasible results that are easily generalizable at the national scale. The HAND predictive flood extent methodology is on the verge of implementation. Hopefully these proposed improvements can further this research, helping to save lives nationwide.

# References


Asquith, W. H. & Roussel, M. H. 2009. Regression Equations for Estimation of Annual Peak-Streamflow Frequency for Undeveloped Watersheds in Texas Using an L-moment-Based, Press-Minimized, Residual-Adjusted Approach. U.S. Geological Survey Scientific Investigations Report 2009-5087. Retrieved from: https://pubs.usgs.gov/sir/2009/5087/pdf/sir2009-5087.pdf

Austin American-Statesman. n.d. History of Onion Creek Flooding. Retrieved from: http://www.statesman.com/news/history-onion-creek-flooding/R6y769kkhg4bo5ZtiesVUM/

Braca, Giovanni, & Futura, Grafiche. 2008. Stage-Discharge Relationships in Open Channels: Practices and Problems. Trento University. Department of Civil and Environmental Engineering.

Brunner, G. W. 2016. HEC-RAS River Analysis System User's Manual Version 5.0. US Army Corps of Engineers, Hydrologic Engineering Center. Retrieved from: http://www.hec.usace.army.mil/software/hec-ras/documentation/HEC-RAS%205.0%20Users%20Manual.pdf

Chow, V. T., Maidment, D. R., Mays, L. W. 1988. Applied Hydrology.

Chow, Ven. 1953. Open-Channel Hydraulics. Civil Engineering Series. The University of Michigan: McGraw-Hill.

City of Austin. n.d. Austin FloodPro. http://www.austintexas.gov/FloodPro/

Cosgrove, B. & Klymmer, C. 2016. National Water Model. Retrieved from: http://water.noaa.gov/about/nwm

Dingman, S. L. 2007. Analytical Derivation of At-a-station Hydraulic-Geometry Relations. Journal of Hydrology 334. DOI: http://dx.doi.org/10.1016/j.jhydrol.2006.09.021

Fagan, C. 2016. Improving Flood Preparedness in South-Central Texas. MA Thesis, University of Texas at Austin. Retrieved from: https://repositories.lib.utexas.edu/bitstream/handle/2152/38755/FAGAN-THESIS-2016.pdf?sequence=1

Federal Emergency Management Agency (FEMA). 2013. NGVD → NAVD? Retrieved from: https://www.fema.gov/media-library-data/20130726-1755-25045-0634/ngvd_navd.pdf

Federal Emergency Management Agency (FEMA). n.d. Flood Map Service Center. Retrieved from: https://msc.fema.gov/portal/

Ferguson, R. 1986. Hydraulic and hydraulic geometry. Progress in Physical Geography 10, 1-31.

Gharari, S., Hrachowitz, M., Fenicia, F., & Savenije, H. H. G. 2011. Hydrological Landscape Classification: Investigating the Performance of HAND Based Landscape Classifications in a Central European Meso-Scale Catchment. Hydrology and Earth System Sciences, 15(11), 3275-3291. Retrieved from: http://www.hydrol-earth-syst-sci.net/15/3275/2011/hess-15-3275-2011.pdf

Gleason, C. J. 2015. Hydraulic geometry of natural rivers: A review and future directions. Progress in Physical Geography, 39(3), 337-360.

Hernandez, W. J., Armstrong, R. A. 2016. Deriving Bathymetry from Multispectral Remote Sensing Data. Journal of Marine Science and Engineering, 4(1), 8. Retrieved from: https://pdfs.semanticscholar.org/cef7/4efb22f8e51b17e16c51f3a1802b1041a561.pdf

Homer, C.G., Dewitz, J.A., Yang, L., Jin, S., Danielson, P., Xian, G., Coulston, J., Herold, N.D., Wickham, J.D., & Megown, K. 2015. Completion of the 2011 National Land Cover Database for the Conterminous United States – Representing a Decade of Land Cover Change Information. Photogrammetric Engineering and Remote Sensing, v. 81, no. 5, p. 345-354

Johnson, M., Ruess, P., & Coll, J. 2016. OPERA – Operational Platform for Emergency Awareness: Reimagining Disaster Alerts. Ch. 13. Consortium of Universities for the Advancement of Hydrologic Sciences, Inc. DOI: http://dx.doi.org/10.4211/technical.20161019

Leopold, L. and T. Maddock 1953. The hydraulic geometry of stream channels and some physiographic implications. Geological Survey professional paper 252, 1-56.

Liu, Y. et al. 2016. A CyberGIS Approach to Generate High-Resolution Height Above Nearest Drainage (HAND) Raster for National Flood Mapping. Retrieved from: http://www.cigi.illinois.edu/yanliu/NFIEHAND.pdf

Liu, Y. Y., Maidment, D. R., Tarboton, D. G., Zheng, X., & Wang, S. W. 2017. A CyberGIS Integration and Computation Framework for High-Resolution Continental-Scale Flood Inunundation Mapping. Journal of the American Water Resources Association (JAWRA). Draft for review.

Maidment, D. R. 2016. Conceptual Framework for the National Flood Interoperability Experiment. Journal of the American Water Resources Association. Retrieved from: https://www.cuahsi.org/Files/Pages/documents/13623/nfieconceptualframework_revised_feb_9.pdf

Manning, R. 1891. On the Flow of Water in Open Channels and Pipes. Transactions of the Institution of Civil Engineers of Ireland. 20. 161-207

Manning, R. 1895. On the Flow of Water in Open Channels and Pipes – Supplement to a Paper Read on the 4th December 1889, published in the Transactions, 1891, vol.

XX, p. 161. Transactions of the Institution of Civil Engineers of Ireland, 24, 179-207

Mckay, L., Bondelid, T., Dewald, T., Johnston, J., Moore, R., & Rea, A. 2012. NHDPlus Version 2: User Guide. Horizon Systems Corporation. Retrieved from: ftp://ftp.horizon-systems.com/nhdplus/NHDPlusV21/Documentation/NHDPlusV2_User_Guide.pdf

Moore, M. R. 2011. Development of a High-Resolution 1D/2D Flood Simulation of Charles City, Iowa. MS Thesis, University of Iowa. Retrieved from: http://ir.uiowa.edu/cgi/viewcontent.cgi?article=2417&context=etd

National Flood Interoperability Experiment (NFIE). n.d. Index of /nfiedata/. http://nfie.roger.ncsa.illinois.edu/nfiedata/

National Oceanic and Atmospheric Administration (NOAA). 2016. NOAA Launches America's First National Water Forecast Model. Retrieved from: http://www.noaa.gov/media-release/noaa-launches-america-s-first-national-water-forecast-model

National Water Model (NWM) Forecast Viewer. 2016. Hydroshare. Retrieved from: https://apps.hydroshare.org/apps/nwm-forecasts/

National Weather Service (NWS). 2016. Natural Hazards Statistics. Retrieved from: http://www.nws.noaa.gov/om/hazstats.shtml

National Weather Service (NWS). n.d. National Forecasts: River Forecasts. Retrieved from: https://water.weather.gov/ahps/forecasts.php

Nobre, A. D. 2011. Height Above the Nearest Drainage – A Hydraulically Relevant New Terrain Model. Journal of Hydrology, 404.1-2, pp. 13-29. DOI: http://dx.doi.org/10.1016/j.jhydrol.2011.03.051

Park, C. C. 1977. World-wide variations in hydraulic geometry exponents of stream channels: An analysis and some observations. Journal of Hydrology, 33, 133-146

Parker, G. 1979. Hydraulic Geometry of active gravel rivers. Journal of Hydraulic Division 105, 1185-1201.

Raymond, P. A. 2012. Scaling the Gas Transfer Velocity and Hydraulic Geometry in Streams and Small Rivers. Journal of Hydrology, 2.1, pp. 41-53. DOI: http://dx.doi.org/10.1215/21573689-1597669

Reistad, K. S., Petersen-Øverleir, A., Bogetveit, L. J. 2005. Setting up Rating Curves Using HEC-RAS. Retrieved from: https://www.researchgate.net/publication/265166848_Setting_up_rating_curves_using_HEC-RAS

Rennó, C. D., Nobre, A. D., Cuartas, L. A., Soares, J. V., Hodnett, M. G., Tomasella, J., & Waterloo, M. J. 2008. HAND, a New Terrain Descriptor Using SRTM-DEM: Mapping Terra-Firme Rainforest Environments in Amazonia. Remote Sensing of Environment, 112(9), 3469-3481. Retrieved from: http://www.dpi.inpe.br/referata/arq/_2012/12_Gabriel/Renno_etal_2008.pdf

Rhodes, D. D. 1977. The b-f-m diagram: Graphical representation and interpretation of at-a-station hydraulic geometry. Amercian Journal of Science 277, 73-96

Rhodes, D. D. 1987. The bfm diagram for downstream hydraulic geometry. Geografiska Annaler. Series A. Physical Geography, 147-161.

Sauer, V. B. 2002. Standards for the Analysis and Processing of Surface-Water Data and Information using Electronic Methods (No. 2001-4044). United States Geological Survey

Seaber, P. R., Kapinos, F. P., and Knapp, G. L. 1987. Hydrologic Unit Maps. U.S. Geological Survey Water-Supply Paper 2294. Retrieved from: https://pubs.usgs.gov/wsp/wsp2294/pdf/wsp_2294_a.pdf

Smith, L. C., Pavelsky, T. M. 2008. Estimation of River Discharge, Propagation Speed, and Hydraulic Geometry from Space: Lena River, Siberia. Water Resources Research 44.3. DOI: http://dx.doi.org/10.1029/2007WR006133

Tarboton, D. G., Idaszak, R., Horsburgh, J. S., Heard, J., Ames, D., Goodall, J. L., ... & Hooper, R. 2014. HydroShare: advancing collaboration through hydrologic data and model sharing. Retrieved from: http://scholarsarchive.byu.edu/cgi/viewcontent.cgi?article=1005&context=iemsscconference

United States Geological Survey (USGS). n.d. Water Watch. Retrieved from: http://waterwatch.usgs.gov

Wahlstrom, M., and Guha-Sapir, D. 2015. "The Human Cost of Weather-Related Disasters 1995-2015." Geneva, Switzerland: UNISDR (2015). Retrieved from: http://www.preventionweb.net/publications/view/46796

Whiteaker, T. 2016. PyNWM. Github Repository. Retrieved from: https://github.com/twhiteaker/pynwm

Zheng, X. 2015. Hydraulic Fabric: An Information Framework for River Channel Cross Section Data. MS Thesis, University of Texas at Austin. Retrieved from: http://hdl.handle.net/2152/31786

Zheng, X., Tarboton, D., Maidment, D., Liu, Y., Passalacqua, P. 2017. River Channel Geometry and Rating Curve Estimation Using Height Above the Nearest Drainage. Manuscript in preparation.

# Vita

Paul Ruess grew up in Northern Virginia, just outside of Washington, D.C. After receiving a Bachelor of Science degree in Civil and Environmental Engineering from the University of Virginia, Paul began a professional career as a wastewater engineer. Paul then moved to Austin one year later to pursue a Master of Science degree in Environmental and Water Resources Engineering. Following graduation, Paul intends to begin a PhD program at the University of Illinois Urbana-Champaign, where he will investigate the Food-Energy-Water Nexus.

Permanent email: pjruess@gmail.com

This thesis was typed by Paul Joseph Ruess.